VOLUME 21, 1959/60, No. 12 pp. 349-376 Published 24th October 1960

Philips Technical Review

DEALING WITH TECHNICAL PROBLEMS
RELATING TO THE PRODUCTS, PROCESSES AND INVESTIGATIONS OF
THE PHILIPS INDUSTRIES

AN ACOUSTIC SPECTRUM ANALYSER WITH ELECTRONIC SCANNING

by D. J. H. ADMIRAAL *).

534.441.2

In 1957 the Institute for Perception Research was founded at Eindhoven. Here, under the direction of Professor J. F. Schouten, members of the Eindhoven Technische Hogeschool and Philips are carrying out joint investigations in the fields of human perception and reactions and information processing.

It is intended to publish from time to time in this Review articles dealing with the work of this Institute. The first of these articles describes the way in which an acoustic spectrum analyser, originally developed in Philips Research Laboratories many years ago, has been modernized by means of semiconductor diodes and transistors.

For the frequency analysis of rapidly varying sounds, such as speech, a device was developed in Philips Research Laboratories round about 1940 which displays the Fourier spectrum on the screen of a cathode-ray tube [1]). This acoustic spectrum analyser is now in use at the Institute for Perception Research where, having been improved in various respects, it is providing valuable service in such fields of investigation as synthetic speech. For this purpose the instrument has proved just as indispensable as a cathode-ray oscilloscope in general electronic work. Some of the improvements referred to will be dealt with in this article.

First we shall briefly describe the operation of the acoustic spectrum analyser in its original form. The frequency-analysing system consists of 79 tuned circuits. Circuit 1 is tuned to 86.5 c/s, circuit 79 to 7440 c/s. The ratio between the resonant frequencies of every two successive circuits is $1 : \sqrt[12]{2} \approx 1 : 1.06$, i.e. the difference is one semitone. The tuned circuits, each with a resistor in series, constitute a series of filters ($F_1, \ldots F_{79}$, *fig. 1*). The Q of the filters being chosen at $Q = 16$, the bandwidth of each filter is also equal to a semitone. The 79 pass bands are thus contiguous and together cover the major part of the range of speech frequencies. The filter inputs are connected in parallel to the output of an amplifier A, to which the signal v_i to be analysed, originating for example from a microphone, is applied. Connected to the output of each filter is a peak-voltage rectifier; this delivers a direct voltage V_k ($k = 1, \ldots 79$) which is a measure of the sinusoidal component of the sound spectrum covered by the kth filter.

By means of a rotary switch S_1 each of the 79 direct voltages V_k drives in turn a push-pull modulator M. The signal voltage v_s is therefore successively equal to V_1, $V_2, \ldots V_{79}$, V_1, and so on. The push-pull modulator is fed with a voltage obtained from the generator G, whose frequency is about 50 kc/s. Depending on the magnitude of the signal voltage v_s, the modulator passes a smaller or larger fraction of the generator voltage, producing on the oscilloscope O a vertical deflection of corresponding amplitude. The horizontal deflection is produced by the voltage divider B and the rotary switch S_2, which turns synchronously with S_1. The switches rotate at 25 revolutions per second, so that all 79 filters are switched in at intervals of $\frac{1}{25}$th second.

If a purely sinusoidal voltage, whose frequency f lies in the middle of one of the 79 pass bands, is applied to the input of the signal amplifier, the signal voltage v_s to the modulator will have the waveform shown in *fig. 2a* (the switch S_1 momentarily breaks circuit between each two successive contacts, caus-

*) Institute for Perception Research, Eindhoven.

1) H. G. Beljers, A recording apparatus for the analysis of the frequency of rapidly varying sounds, Philips tech. Rev. 7, 50-58, 1942.

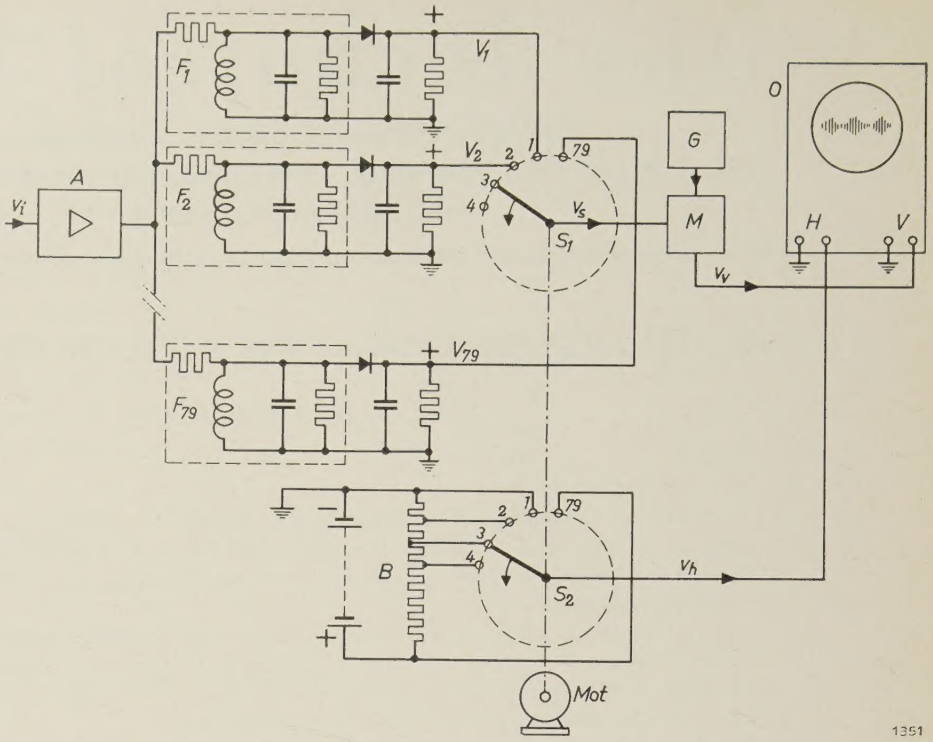

Fig. 1. Basic circuit diagram of Beljers' acoustic spectrum analyser [1]). *A* signal amplifier. F_1, ... F_{79} filters which divide the frequency range from 86.5 to 7440 c/s into 79 consecutive frequency bands, each a semitone in width, and each provided with a peak-voltage rectifier. *G* generator (frequency approx. 50 kc/s). *M* push-pull modulator, which passes more of the generator voltage the higher is the signal voltage v_s; this signal voltage is the rectified output of the filters, which are consecutively connected to *M* via the rotary switch S_1. The output voltage v_v of *M* causes the vertical deflection on the oscilloscope *O*. The horizontal deflection is produced by a pulsed voltage v_h (see fig. 2*c*) derived from the voltage divider *B* via the rotary switch S_2. Both switches, S_1 and S_2, are mounted on the same shaft, driven by the motor *Mot*.

ing v_s to drop momentarily to zero). It can be seen that, in addition to the filter in whose passband the signal frequency f lies, the neighbouring filters also deliver a voltage. The resultant vertical deflection voltage v_v from the modulator is thus as shown in fig. 2*b*. The horizontal deflection voltage v_h is shown in fig. 2*c* (switch S_2 also breaks circuit between successive contacts; for simplicity it is assumed here that there are only 17 filters). The oscillogram (spectrogram) takes the shape shown in fig. 2*d*, which recalls the deflection pattern produced by a vibrating-reed frequency meter.

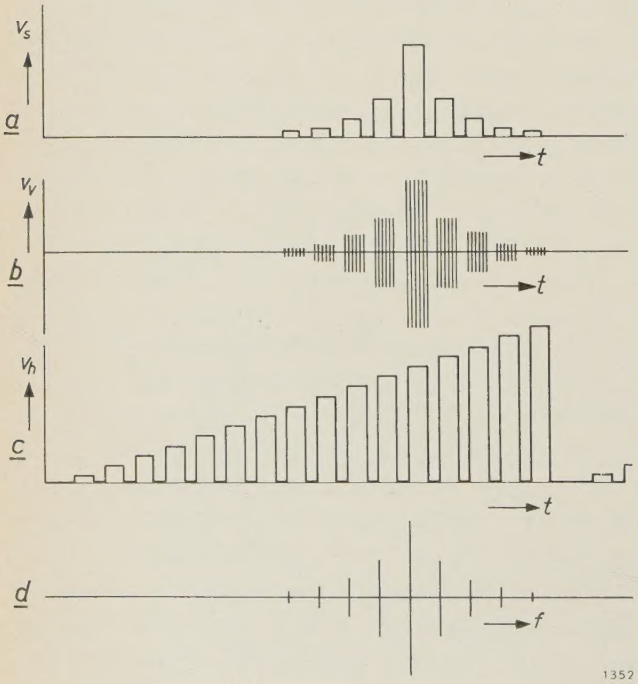

Fig. 2. *a*) Form of the signal voltage v_s in fig. 1, for a sinusoidal input signal.
b) Corresponding form of the output voltage v_v from the modulator.
c) Pulsed sweep voltage v_h (for simplicity shown here for 17 filters instead of 79).
d) Form of the oscillogram. At the peak of each pulse (*c*), v_h is constant for a moment, during which time a vertical line is traced, the length of which corresponds to v_v in (*b*).

The fact that a sinusoidal signal does not produce a single-line spectrum, but a spectrum as shown in fig. 2*d*, limits the resolving power of this spectrum analyser. A discussion of this subject, and its relation to the *Q* of the filter circuits and the time constant of the smoothing circuits, will be found in the article mentioned under [1]).

The principal modification of the original apparatus is the replacement of the rotary switches by electronic switches. These have the advantage of being entirely free from mechanical noise, a point of particular importance in acoustic experiments. Furthermore, they preclude troubles due to bad contacts, which are always a drawback of rotary switches in the long run.

A photograph of the acoustic spectrum analyser in its present form is shown in *fig. 3*.

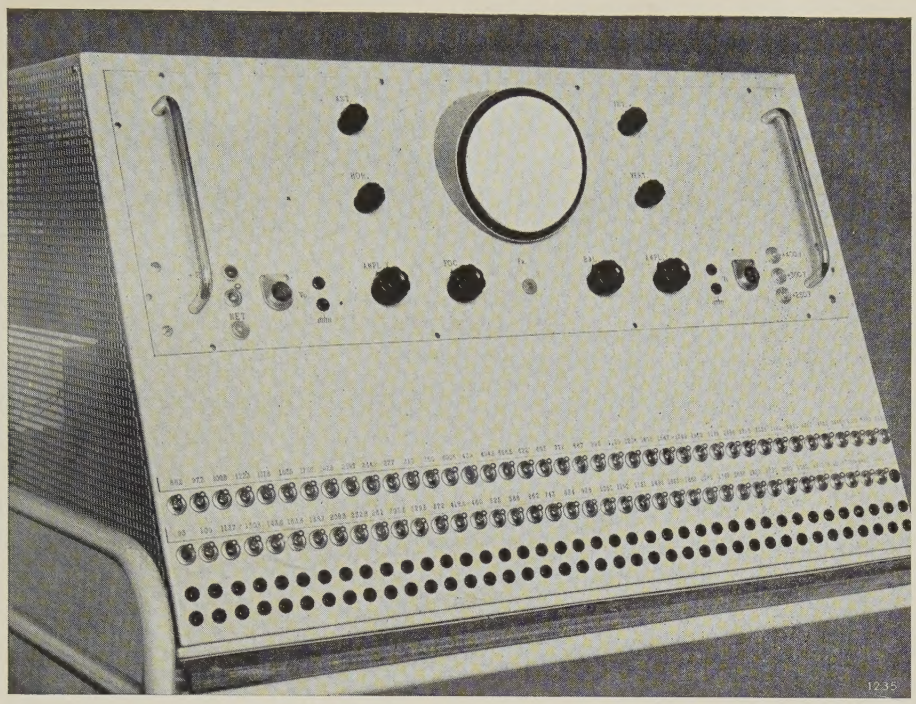

Fig. 3. The Beljers acoustic spectrum analyser in its present form at the Institute for Perception Research at Eindhoven.

Replacement of the rotary switch S_1

Each contact of the rotary switch S_1 is replaced by a diode switch, driven by a transistor circuit. The principle of the diode switch is illustrated in *fig. 4a*. In the state represented, the cathode of the diode D is at a positive potential in relation to the anode, and therefore the diode passes no current. The output voltage V_o of the circuit is then $R_o/(R_o + R)$ times the input voltage V_i. If, on the other hand, the cathode is earthed (for the present we assume this to be done by the switch Q), the diode then constitutes a virtual short-circuit across the resistor R_o, so that $V_o \approx 0$.

In principle, 79 of these electronic switches can replace the rotary switch S_1 in fig. 1. V_i is the rectified voltage V_k of one of the 79 filters, and the output V_o represents the voltage v_s that drives the modulator. (In this case, since $R = R_o$, v_s is not equal to V_k but to $\frac{1}{2}V_k$.) This means that measures must be taken to raise the cathode potential successively to a positive value in each of the 79 diode circuits.

Before discussing these measures, we must elaborate somewhat on the circuit of fig. 4*a*. In the state when the cathode is earthed the diode is not a complete short-circuit across R_o, and therefore v_s is not entirely zero. The result of this would be a spurious background in the spectrogram. The residual value of v_s can be reduced to zero, however, by instead of merely earthing the cathode of D, giving it a small negative bias — large enough to achieve the object, but not too large since that would make the residual value of v_s negative and again

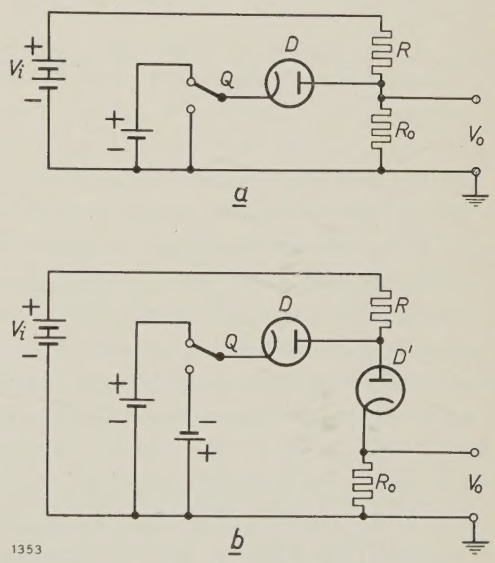

Fig. 4. *a*) When the cathode of diode D is positively biased at a potential higher than the potential drop across R_o, the diode is cut off. The output voltage V_o is then $R_o/(R_o + R)$ times the input voltage V_i. If the cathode is earthed, D constitutes a virtual short-circuit across R_o, and V_o drops almost to zero. *b*) By adding the diode D' the voltage V_o — when D is conducting — can be made exactly zero with the aid of a negative bias on the cathode of D, the value of which is not critical.

give rise to unwanted deflections. Unfortunately the appropriate bias is not identical for all diodes of the same type. Nevertheless, it is possible to make do with a single bias-voltage source for all 79 electronic switches by connecting a diode D' in series with R_0 (fig. 4*b*). This prevents current flowing through R_0 in the wrong direction, and as a result the residual value of v_s can no longer go negative. This allows us to raise the common negative bias to a point where the voltage v_s drops to zero in that electronic switch where it has the highest positive residual value; in the other switches the negative bias is higher than is necessary, but this can do no harm because of the presence of the diodes D'.

Fig. 5 shows a three-fold arrangement of the circuit in fig. 4*b*, provided with one common resistance R_0. The negative bias is applied to points Q_1, Q_2 and Q_3. If these points are given successively a certain positive potential, then v_s becomes successively about $\frac{1}{2}V_1$, $\frac{1}{2}V_2$ and $\frac{1}{2}V_3$.

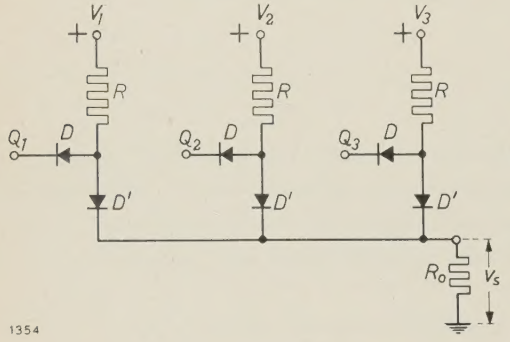

Fig. 5. The circuit of fig. 4*b*, now with three inputs and one common output resistor R_0. The diodes are semiconductor diodes.

To produce this circuit with 79 inputs we need 2×79 diodes. This makes the use of semiconductor diodes, as in fig. 5, highly desirable because of their much smaller heat development and because they dispense with the need for heater-current leads.

In order to produce the various sinusoidal components in their correct ratios in the spectrogram we must ensure that the ratio $v_s : V_k$ is independent of the applied voltage V_k. If the diodes D' were ideal (resistance R_i in the forward direction $= 0$, resistance R_{inv} in the inverse direction infinite), this condition would be fulfilled, because in that case $v_s/V_k = R_0/(R_0 + R) =$ constant. In practice, however, we must replace R in this expression by $R + R_i$, and R_0 by the parallel arrangement of R_0 and $R_{inv}/78$. The resistance R_i depends on the current through the diode (and hence on R), and R_{inv} depends on the voltage across the diode. To minimize the effect of R_i we must make R much larger than the value of R_i, i.e. $R \geqq 100$ kΩ for a germanium diode, type OA 74, and $R \geqq 220$ kΩ for a silicon diode, type OA 202. To prevent v_s becoming much smaller than V_k, we make, as mentioned above, $R_0 = R$, that is to say $v_s \approx 0.5\ V_k$.

To neutralize the influence of R_{inv} we must ensure that $\frac{1}{78}\ R_{inv}$ is much larger than R_0. With $V_k = 10$ V the inverse voltage across 78 diodes D' is approx. 5 V. At this voltage, 78 germanium diodes of type OA 74 in parallel have a resistance of only about 50 kΩ. This is appreciably less than R_0, which must be at least 100 kΩ. In this respect silicon diodes, type OA 202, are much better: 78 of these in parallel at 5 V have a resistance of approx. 70 MΩ, which is very much larger than $R_0 = 0.22$ MΩ. For this reason we decided to use silicon diodes, with $R = R_0 = 220$ kΩ.

Fig. 6 shows the relation $v_s = f(V_k)$ measured for the above-mentioned arrangement. The relation is virtually linear for values of V_k larger than 0.3 V. The required proportionality between v_s and V_k is adequately approached if a bias of 0.3 V is added to V_k.

In order that the diode circuits of fig. 5 — provided with 79 inputs — shall each in turn pass the rectified filter voltages V_k to the output (with a reduction factor of approx. $\frac{1}{2}$), the points Q_1, Q_2, ... Q_{79} must receive successively a specific positive voltage, and during the rest of the time remain at the negative potential mentioned above. This is done automatically by means of a flip-flop circuit connected to each diode D; this arrangement is illustrated in *fig. 7*. The 79 flip-flop circuits are identical and are coupled one with the other to form a ring circuit. They are supplied with a direct voltage of approx. 12 V.

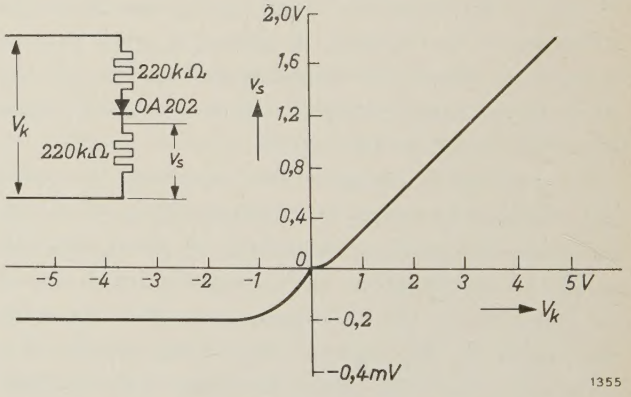

Fig. 6. Output voltage v_s as a function of the input voltage V_k for the circuit on the left, using a silicon diode OA 202. In the forward direction the relation is linear for $V_k > 0.3$ V. (Note the different scales of the positive and negative v_s axes.)

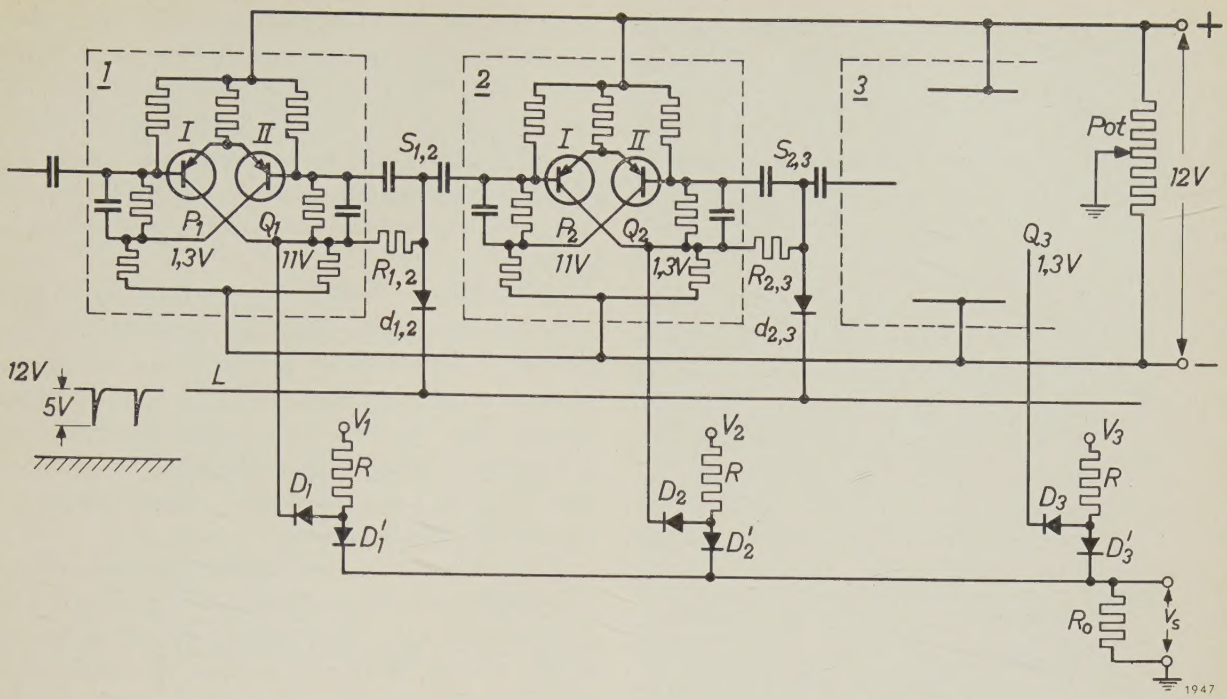

Fig. 7. The diodes D_1, D_2, D_3, ... are driven by 79 flip-flop circuits *1*, *2*, *3*, ... Flip-flop *1* is here in the "activated" state (transistor *I* conducting, *II* cut off, Q_1 is at the "high" potential, D_1 is cut off, $v_s = \frac{1}{2}V_1$). The other flip-flop circuits are in the quiescent state (transistor *I* cut-off, *II* conducting, Q_2, ... Q_{79} are at the "low" potential, D_2, ... D_{79} are all conducting, so that V_2, ... V_{79} make no contribution to v_s). The successive flip-flop circuits are consecutively triggered by negative pulses on the line L.

Each flip-flop is provided with two transistors, type OC 71. There is always one flip-flop in the "activated" state whilst the other 78 are in the "quiescent" state. "Activated" means here that transistor *I* is conducting and transistor *II* non-conducting; point *P* thereby has a potential of 1.3 V and point *Q* a potential of 11 V in relation to the negative line. In the quiescent state the reverse is the case: transistor *I* is non-conducting, *II* conducting, *P* is at 11 V and *Q* at 1.3 V with respect to the negative line.

Points $Q_1, Q_2, \ldots Q_{79}$ are the corresponding points of the diode circuits (cf. fig. 5). Thus, only that diode circuit is operative whose associated flip-flop circuit is in the activated state; the voltages indicated in fig. 7 are for flip-flop *1* in the activated state.

The potentiometer *Pot*, the sliding contact of which is earthed, is adjusted so that the "low" voltage of all points *Q* with respect to earth has just the value needed in order to suppress the residual values of the voltage v_s across R_0 (see above). The "high" voltage of Q_1 with respect to earth (switch *1* being activated) is then still high enough to block diode D_1 completely, v_s then being approximately equal to $\frac{1}{2}V_1$.

The points $S_{1,2}$, $S_{2,3}$ etc. between the successive flip-flop circuits are connected via diodes $d_{1,2}$, $d_{2,3}$ etc. to a line L. With respect to the negative pole this has a potential of 12 V, superimposed on which are negative triggering pulses of approx. 5 V having a frequency of 2000 c/s. The anode of $d_{1,2}$ is connected via a resistor $R_{1,2}$ to Q_1, that of $d_{2,3}$ via $R_{2,3}$ to Q_2, and so on. The triggering pulses therefore find all diodes blocked except $d_{1,2}$ (since only Q_1 has the "high" voltage of 11 V). Via $d_{1,2}$ and the two coupling capacitors there thus arrives a negative pulse on the base of transistor *II* in flip-flop *1* and on the base of transistor *I* in flip-flop *2*. Both these circuits therefore change their state: *1* goes over into the quiescent state and *2* into the activated state. Upon the arrival of the next triggering pulse the same happens to *2* and *3*, and so on. In this way, the activated state passes $2000/79 \approx 25$ times per second around the ring of flip-flop circuits and successively makes each of the 79 diode circuits momentarily conductive.

When flip-flop *2*, for example, changes to the activated state (fig. 7), the voltage of Q_2 jumps from 1.3 V to 11 V. The latter value is reached before the triggering pulse has ended, and there is therefore a danger that diode $d_{2,3}$ will open and cause the premature activation of flip-flop *3*. To prevent this happening, measures are taken to cause the anode voltage of $d_{2,3}$ to follow the voltage jump of Q_2 so slowly that $d_{2,3}$ remains blocked during the pulse. This means that the voltage variation on the anode of $d_{2,3}$ must have a sufficiently large time constant. (This time constant is determined primarily by the resistance $R_{2,3}$ and the capacitance of the coupling capacitors.) This applies, of course, to all 79 coupling networks.

The triggering pulses are derived by differentiation from a square-wave voltage generated by a multivibrator, using a double triode, type E 88 CC. Between the multivibrator and the line L a transistor type OC 77 is connected as an emitter-follower for matching between the impedances.

Replacement of the rotary switch S_2

A pulsed sweep voltage, like that obtained from the rotary switch S_2 (fig. 1) for the horizontal deflection (fig. 2*c*), is not easy to produce by electronic means. Other waveforms can be used, however, such as a staircase or a sawtooth waveform. A staircase voltage is again difficult to produce electronically [2]), whereas a sawtooth voltage is fairly simple to generate. *Fig. 8a* shows the appearance of

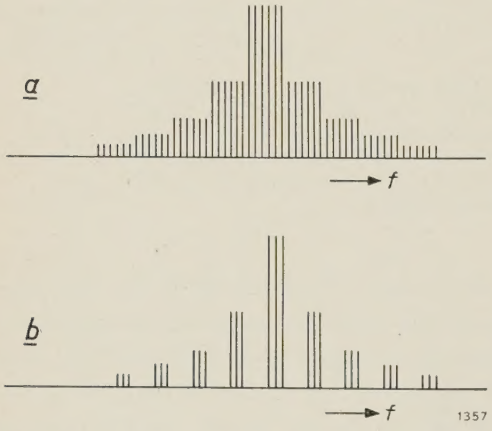

Fig. 8. *a*) Form of the spectrum of a sinusoidal voltage when the horizontal deflection is produced by a sawtooth voltage. *b*) The same, but now with the electron beam of the C.R.T. periodically suppressed for $\frac{1}{4}$ ms each $\frac{1}{2}$ ms by means of a square-wave voltage of 2000 c/s applied to the control grid of the oscilloscope. Each "bar" is in fact a sine wave train of about 12 cycles of the 50 kc/s voltage, but appears to the eye as a single vertical line.

a spectrogram of a sinusoidal signal when a sawtooth voltage is used for the horizontal deflection. A spectrogram of this kind is just as useful as the line spectrum obtained with the original apparatus (fig. 2*d*), but it is somewhat less suggestive. For this reason an attempt has been made to approximate to the latter spectrum in the following way. The oscilloscope tube is kept just below cut-off by a negative bias on the control grid, but the beam suppression is lifted once in every half cycle by a square-wave strobe voltage of 2000 c/s applied to the same electrode; this strobe voltage is derived from the multivibrator mentioned above. During every half millisecond, therefore, the electron beam is present for only $\frac{1}{4}$ millisecond. The effect of this on the spectrogram of a sinusoidal signal is shown in fig. 8*b*. The individual "bars" are not sharp lines as in fig. 2*d*, but sinusoidal wave trains of about 12 cycles of the voltage from generator G (fig. 1), which has a frequency of about 50 kc/s; the difference, however, is scarcely perceptible in practice.

The sawtooth voltage is generated by a Miller integrator based on a transitron-connected pentode (EF 80) [3]). Free-running the circuit has a frequency of approx. 20 c/s. When the 79th flip-flop circuit returns from the activated to the quiescent state, it produces pulses with a repetition frequency of $2000/79 \approx 25$ per second; these pulses are used to synchronize the transitron.

It is necessary to make the flyback time as short as possible since the information delivered by the filter circuits that come into operation during the flyback is lost. With this in view the capacitor in the sawtooth generator is made to charge up extremely rapidly through a cathode follower (one half of a double triode E 88 CC), which is driven by the transitron-Miller. In this way the flyback time has been reduced to less than 0.25 ms, i.e. less than 0.6% of the sawtooth period. (In a normal sawtooth generator the flyback time is generally about 10%.)

The short flyback time gave rise to a difficulty which, however, it proved possible to overcome completely. The difficulty is most evident if the input signal is a sinusoidal voltage with a frequency of 7440 c/s (the resonance frequency of the 79th filter network). The spectrogram then appears as illustrated in *fig. 9*. The deflections on the left of the spectrum create the false impression that the input signal also contains low-frequency components. This is particularly troublesome if the input signal really possesses a complicated spectrum.

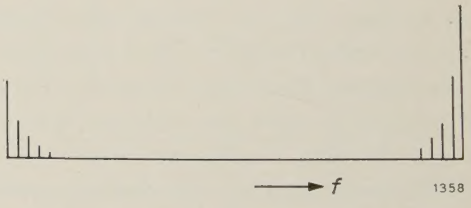

Fig. 9. Spectrogram of a sinusoidal voltage of frequency 7440 c/s. The deflections on the left suggest the presence of low-frequency components. They are due to the stray capacitance in parallel with R_0 being unable to discharge rapidly enough (cf. fig. 10).

[2]) See e.g. Philips tech. Rev. **12**, 288, 1950/51.

[3]) A transitron circuit is one of the pentode circuits with which a negative resistance is obtained; see for example F. E. Terman, Radio Engineer's Handbook, McGraw-Hill, London 1950, p. 318. A Miller integrator based on a transitron (see e.g. F. Kerkhof and W. Werner, Television, Philips Technical Library, 1952, p. 138 *et seq.*) produces a sawtooth generator that gives a very linear sawtooth wave-form.

The effect is due to the presence of an appreciable stray capacitance C_p in parallel with the resistor R_o across which the signal voltage v_s for the modulator appears. (This stray capacitance consists mainly of wiring capacitance and the total capacitance of the diodes connected to R_o.) The measured value of C_p was about 1500 pF, and with $R_o = 220$ kΩ this gives a time constant R_oC_p of 0.33 ms. In the flyback time of about 0.25 ms the voltage across C_p therefore drops only in the ratio of $1 : e^{-0.25/0.33} = 1 : 0.47$, and the deflection at the extreme left will consequently still be almost half as large as the deflection at the extreme right.

In principle the unwanted deflection on the left can be reduced in the following ways:

1) By reducing C_p; this, however, proved to be impracticable.
2) By reducing R_o, though at the expense of sensitivity.
3) By lengthening the flyback time, which would mean losing part of the spectrum; to remedy this, the ring would have to be extended by some additional flip-flop circuits.
4) By making C_p discharge rapidly during the flyback with the aid of some kind of switch.

The latter method proved to be a satisfactory solution. The switch used is a transistor (*fig. 10*) which is normally in the cut-off state but is made to conduct momentarily by the synchronizing pulse to the sawtooth generator during every flyback; this pulse originates from the 79th flip-flop circuit. The polarity of the voltages makes it necessary to use an *N-P-N* transistor, type OC 139.

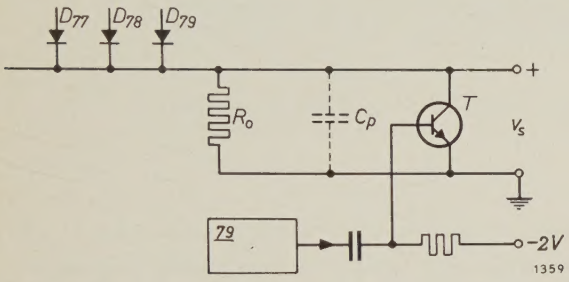

Fig. 10. The stray capacitance C_p (approx. 1500 pF) in parallel with the resistor R_o (220 kΩ) is rapidly discharged, during the flyback, through the transistor T (*N-P-N* transistor, type OC 139) which is periodically made to conduct by synchronizing pulses applied to its base. The synchronizing pulses are taken from the 79th flip-flop circuit. This arrangement suppresses the effect shown in fig. 9. (The diodes should be marked D_{77}', D_{78}', D_{79}'.)

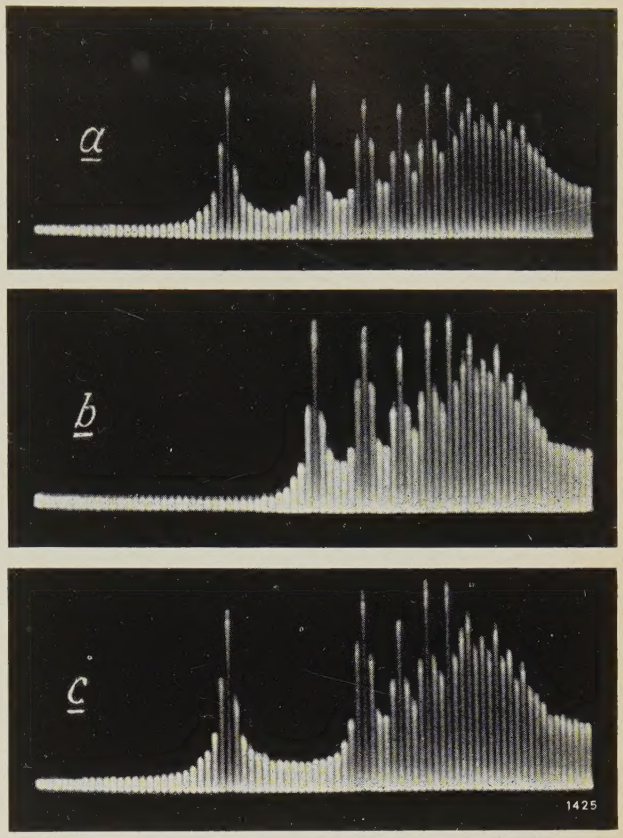

Fig. 11. Examples of spectrograms recorded on the acoustic spectrum analyser described in this article.
a) Fourier spectrum of a pulse.
b) Idem, with suppressed fundamental component.
c) As (*a*), with second harmonic suppressed.

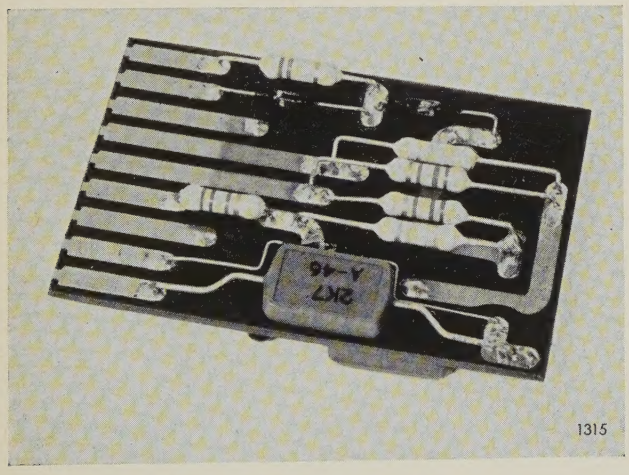

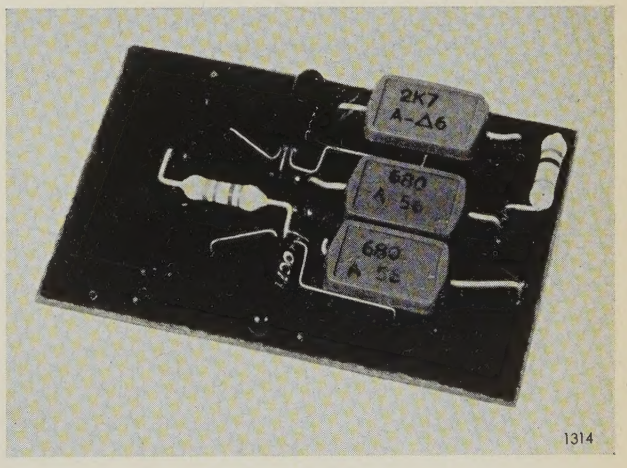

Fig. 12. The two sides of a printed-wiring board (42 × 76 mm), containing a diode switch circuit (D, D' and R), the associated flip-flop circuit and the components for coupling to the next stage. The board is held by spring contact clips, which serve as electrical connections to the rest of the circuit.

Photographs of a number of spectrograms are shown in *fig. 11a, b* and *c*. It will be noticed that (cf. fig. 2*d*) the negative deflections are now suppressed. This has the advantage of allowing the horizontal axis to be lower on the oscilloscope screen, enabling the positive deflections to be made larger.

yser use is made of printed wiring [4]). For example, the 79 diode circuits with their flip-flop circuits are each assembled on a printed-wiring board 42×76 mm (*fig. 12*). The boards are held in place by spring clips which also constitute the electrical contacts. In this way the individual circuits are

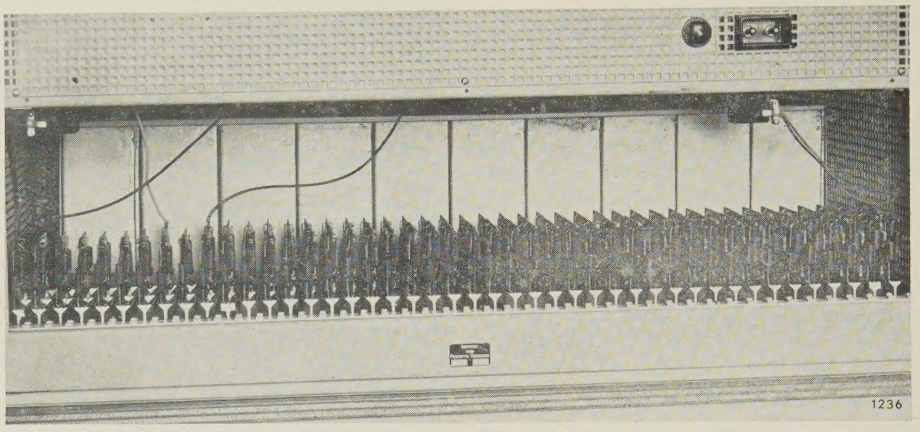

Fig. 13. Rear view of the interior of the acoustic spectrum analyser, showing the printed-wiring boards, one of which appears in fig. 12.

It should be mentioned in conclusion that the full width of the spectrum need not always extend from 86.5 to 7440 c/s; a smaller frequency band can be covered, which can then be displayed over the full width of the screen.

Constructional features

In many circuits of the acoustic spectrum anal-

easily removable for testing and change where necessary. *Fig. 13* shows the boards in position in the apparatus, showing the neat, compact and accessible assembly.

Various pilot lamps are fitted to facilitate the localization of faults.

[4]) See e.g. Philips tech. Rev. **20**, 113, 1958/59.

Summary. Beljers's acoustic spectrum analyser contains 79 filters whose pass bands, each a semi-tone in width, consecutively cover a frequency range from 86.5 to 7440 c/s. In the original apparatus (of 1942) a rotary switch was used for causing each of the filter voltages to produce successive vertical deflections on an oscilloscope, and a second rotary switch was used to make the horizontal deflection increase stepwise logarithmically with the frequency. In the Institute for Perception Research at Eindhoven the apparatus has been modernized, one of the improvements being the replacement of both switches by silently-operating electronic switches using semiconductor diodes and transistors. Use is also made of printed wiring.

A SIMPLE METHOD OF DETERMINING THE THERMAL CONDUCTIVITY OF SOLIDS

by J. SCHRÖDER *).

536.21.08

The remarkable feature of the method described is that it involves no temperature or quantitative heat measurements. The procedure, using a small cylindrical sample, consists merely in taking a stop-watch reading (of a few minutes) and finding a value on a calibration chart.

Unlike many other material properties, the thermal conductivity has been measured on only relatively few solid materials. Moreover, the values reported for one and the same material often show considerable discrepancies, sometimes 50% or more. These discrepancies are partly explained by differences in the composition, degree of purity, pretreatment, etc., of the samples measured. They stem largely, however, from the difficulties involved in measuring this property reliably and reproducibly. These difficulties may also explain why relatively so few solids have been subjected to thermal conductivity measurements, in spite of the growing importance of this property for scientific as well as technical reasons. It is of interest scientifically because no comprehensive theory has yet been put forward to explain the mechanism of (non-metallic) thermal conduction in solids. It is of technical importance in connection with all solid-state applications involving the conversion of thermal energy. In some applications, such as Peltier cooling and thermo-electric energy production, heat conduction in fact governs the efficiency that can be achieved.

The methods of determining thermal conductivity, λ, described in the literature, are too numerous to summarize here [1]). Common to all of them is the measurement of the temperature difference ΔT across a sample of length l — conveniently done with thermocouples — and of the quantity of heat Q flowing through the sample in a given time t. The thermal resistance R is then given by

$$\frac{1}{R} = \frac{A}{l}\lambda = \frac{Q}{t\Delta T}, \quad \ldots . \quad (1)$$

where A is the cross-section of the sample. The value of Q is usually derived from the electric power used for the heat supply, but it can also be measured calorimetrically. The most accurate values of λ are obtained by measurements in the steady state, to which (1) applies. This involves a lengthy measurement, however, since it is necessary to wait until this state is reached, and particularly since, to minimize heat losses, the sample and the heat source must be shielded and the shielding must also be brought to the requisite steady temperature. Moreover, these precautions entail the use of rather cumbersome equipment. In many methods, too, a good deal of time is spent on preparing the sample, so that all in all no more than one sample a day can be investigated.

In the following a new method is described, which uses simple equipment and makes it possible to measure the thermal conductivity of solids at room temperature quickly and accurately. An incidental advantage of the method is that the samples required are not only easy to make but can also be fairly small — a most important requirement where many solids are concerned and one which is certainly not met by certain older methods. The same method, with some supplementary equipment, can also be used for determining λ values at temperatures well above and below ambient, viz. between -200 and $+400$ °C.

The basis of the new method is the maintenance of a fixed temperature difference between the ends of the sample, the temperature of each end being held constant by contact with two boiling liquids. What is measured is the time in which, in the steady state, a certain quantity of heat passes through the sample; this quantity is established quite simple by the quantity of liquid made to evaporate at the "cold" end of the sample.

The principle of the method is illustrated in *fig. 1* [2]). In the lower vessel A a pure liquid a is brought to the boil. The vapour flows over the silver plate S_1, is condensed in the cooler K_1, and the condensate returns through the overflow pipe L into the vessel. In this way, plate S_1 is very effectively kept at a constant temperature, the boiling

*) Zentrallaboratorium Allgemeine Deutsche Philips Industrie GmbH, Aachen Laboratory.

1) See e.g. M. Jakob, Heat transfer, Wiley, New York 1949, Part 1, Chapter 9. Also Archiv für technisches Messen V 9213 1 to 4.

2) The apparatus will shortly be put on the market by Colora Messtechnik GmbH, Lorch/Würtemberg, Germany.

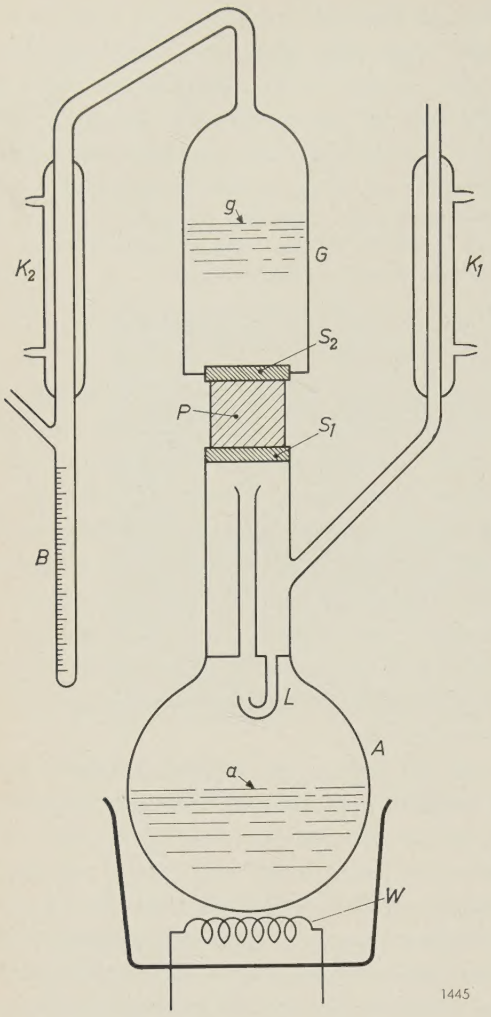

Fig. 1. Principle of the new method of determining the thermal conductivity of solids. P sample of material under investigation. A and G vessels containing two different liquids (a and g). W heating element that keeps a on the boil. S_2 and S_1 silver plates, ensuring good thermal contact of P with the liquid g and the vapour of a, respectively. K_1 condenser and L overflow pipe for returning the condensate of a. The liquid g, whose boiling point is roughly 10 °C lower than that of a, is brought to the boil by the heat transmitted through the sample P. K_2 condenser and B tube, graduated in millilitres, for collecting and indicating the vaporated quantity of liquid g.

point T_a of the liquid, for if S_1 drops only slightly below that temperature, vapour condenses on the plate and transfers to it its heat of condensation, causing the temperature of the plate to rise again to T_a. The upper vessel G contains another pure liquid, g, whose boiling point is, say, 10 °C lower than that of liquid a. At the bottom of this vessel there is another silver plate, S_2. Fitted between the two plates, S_1 and S_2, is a cylindrical sample P of the material under investigation. The heat that flows through this sample from S_1 to S_2 brings the liquid g to the boil, thereby keeping the temperature of S_2 constant at the boiling point T_g of g. Between the two silver plates there is therefore a constant temperature difference $T_a - T_g$. The vapour from liquid g is condensed in the cooler K_2 and the condensate is collected in a tube B, marked with a millilitre scale.

As soon as the steady state of heat flow is reached — which is reached when about 0.1 ml of condensate has collected in B — the time t taken for a certain liquid volume V, say 1 ml, to flow into B is determined with a stop watch. Let S be the heat of vaporization of the liquid g per unit volume, then eq. (1) gives:

$$\lambda = \frac{l}{A}\frac{1}{R} = \frac{l}{A}\frac{VS}{t(T_a - T_g)}. \quad . \quad . \quad . \quad (2)$$

Given the data on the liquids and the dimensions l and A of the sample we can calculate λ from the measured values of V and t.

The method shows a remarkably high degree of accuracy, owing to the fact that the effect of heat losses between S_1 and the liquid g is kept relatively very low. This is done primarily by choosing the dimensions of the sample so as to ensure a reasonably large heat flow through the sample. For instance, if the substance is a poor conductor of heat, the sample taken will be in the form of a thin disc. For a better conductor, assuming the same temperature difference, a thicker sample will be taken, for an unduly large heat flow would cause the liquid g to boil too turbulently, with the risk of liquid splashing over into tube B. Furthermore, if the appropriate quantity of liquid distils too quickly into B, the time measurement is less accurate. The time t should preferably be between 100 and 1000 seconds, and this can be arranged not only by a suitable choice of the thermal resistance of the sample but also by using suitable liquids (fixing the values of S and T_a and T_g).

Heat may be lost from the upper vessel as well as from the sample, causing errors in V through insufficient evaporation or premature condensation. These errors can be minimized by enclosing the upper vessel G in a vacuum jacket (dewar flask); see the photographs of the set-up in *fig. 2*.

The method as described enables absolute determinations of λ to be made. If a number of calibrated samples are available, λ can be determined even more easily by a comparative measurement [3]). The times t found for the calibrated samples are plotted in a diagram against the known values of the thermal resistance R. On the calibration curve thus

[3]) The standard samples were prepared for us by K. H. Bode and W. Fritz of the Physikalisch-Technische Bundesanstalt, Brunswick. The values of thermal resistance determined by them were accurate to within ± 1% (Z. angew. Phys. **10**, 470-479, 1958). We take this opportunity to thank them for their valuable assistance.

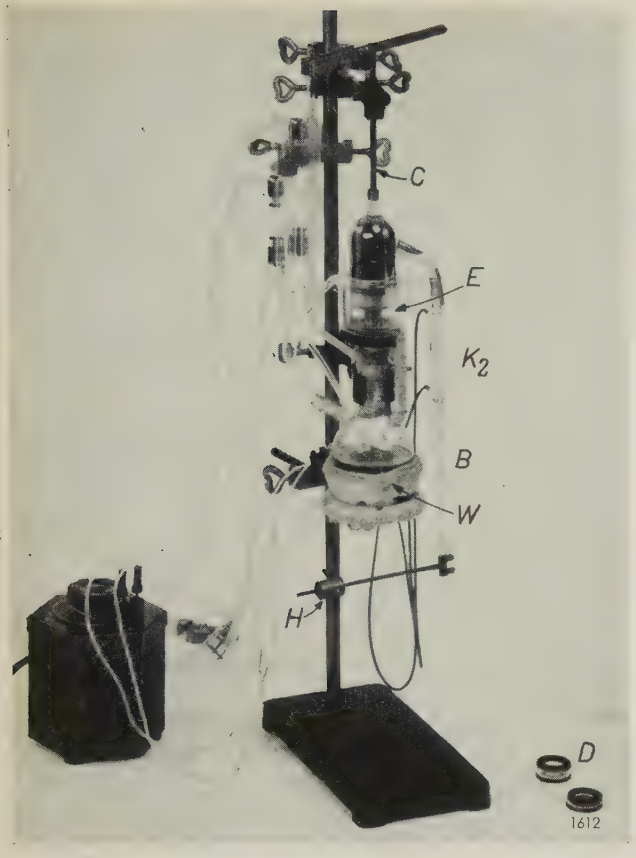

a

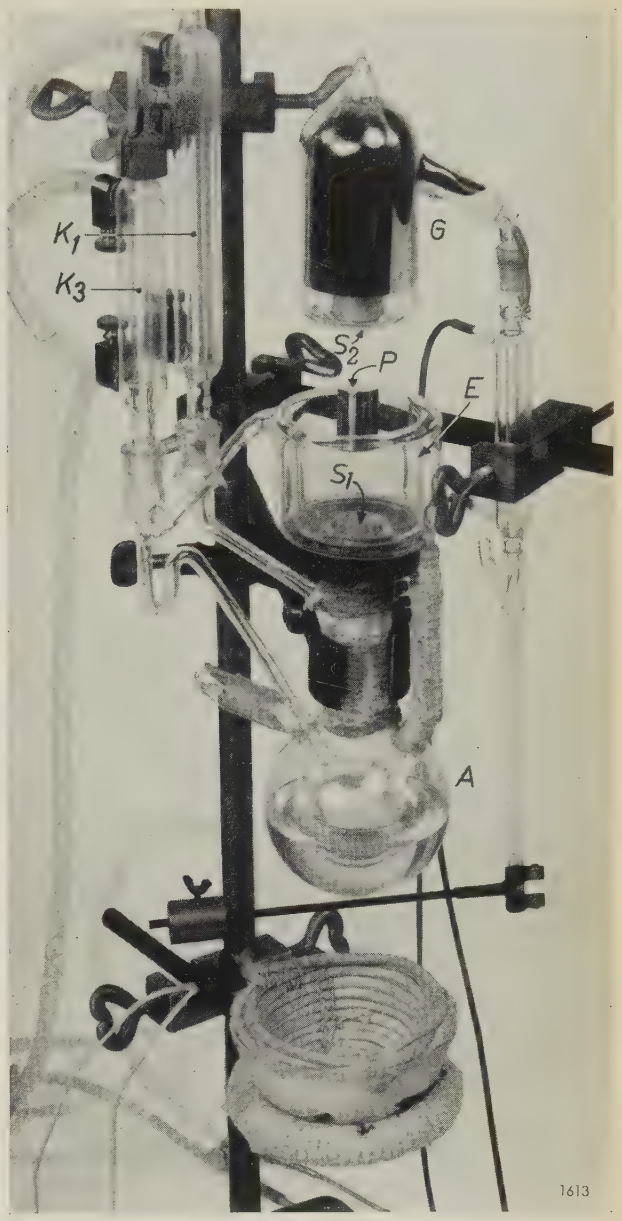

b

Fig. 2. The apparatus, *a*) ready for use, *b*) partially dismantled (for this photograph the sample P was suspended by a thread between the two silver plates S_1 and S_2).

The upper vessel G is in the form of a dewar flask, with the sealed-off pinch at the top and the condenser K_2 and graduated tube B at the side. It is placed over the sample and pressed down by the long helical spring C. K_2 and B are balanced by an arm with the weight H. One of the rings D is placed around the sample to give thermal insulation. A refinement not shown in the arrangement in fig. 1 is a double-walled glass vessel E surrounding the sample; between the walls the vapour can be circulated of a liquid whose boiling point is between those of a and g. The vessel containing this liquid can be seen inside vessel A, and associated with it is a condenser K_3 with return pipe.

obtained we can then, after having measured the time t, read off directly the value of R for a given sample, and from this value, together with the dimensions of the sample, we can calculate the value of λ.

It should be noted that for these relative measurements it is not necessary to know the exact values of V, T_a and T_g. This at once eliminates the errors that can creep into a calculated λ value if *a*) the boiling points T_a and T_g should differ slightly from the assumed values owing to impurity of the liquids, and if *b*) the ends of the sample should not attain the exact temperatures T_a and T_g owing to contact resistances to the heat transfer between the silver plates and the sample. It should of course be ensured that these resistances are equal for all measurements, in order to obtain reproducible results. The same applies to the magnitude of the small residual heat loss, to which we shall return presently.

The calibration curve, as can be seen in *fig. 3*, is very closely a straight line. The negligible spread of the points is evidence of the high degree of reproducibility of which the method is capable. According to eq. (1) the curve should be a straight line through the origin. In the diagram this is not so, the line cutting off a section R_0 on the ordinate axis. This corresponds to the thermal resistance of the various heat-transfer surfaces. For each pair of liquids used the calibration line must be plotted afresh, but since it is a straight line it is sufficient to measure two standard samples, possibly with a third for verification.

By this comparative method, a measurement, including the preparation, lasts no more than 5 to 15

minutes. The error of measurement is ± 3% at the most. No temperatures need be measured, and it is not necessary to know the exact values of the boiling point and heat of vaporization of the liquids used. The liquids need not even be pure, provided the same liquids are used for calibration and measurement. The ease and speed with which a sample can be measured by this method open up the practical possibility of investigating systematically large series of specimens, as for example mixed crystals of varying composition.

Some particulars follow concerning the equipment and the samples.

Various measures are taken to ensure that the temperatures of the silver plates S_1 and S_2 will be accurately reproducible. To avoid any delayed-boiling effect in liquid g, capillary holes are made in the plate S_2. To increase the surface area for the heat transfer, both plates S_1 and S_2 are provided with grooves on the side in contact with the vapour and liquid, respectively. At the other side the plates are ground flat to obtain the best possible contact between sample and plates; also, the sample length is thereby precisely defined. To reduce the contact resistances a heat-transfer fluid is applied between the faces, and the plates are held against the sample under considerable (and constant) spring pressure (see fig. 2*a*). In this way the variations in the thermal resistance across the heat-transfer surfaces are reduced to such an extent that their effect in all measurements remains below the limits of accuracy determined by other factors.

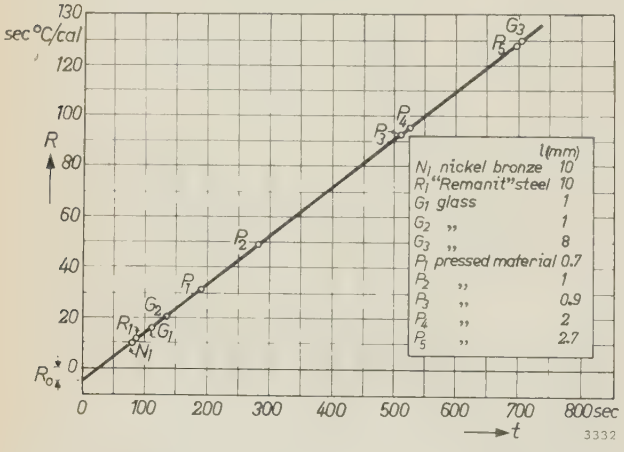

Fig. 3. Calibration chart for an apparatus using carbon disulphide and ether as boiling liquids (boiling points 46.3 and 34.5 °C, respectively). For ten calibrated samples (see inset) for which the thermal resistances R were known — values differing by a factor 10 for these samples — R is plotted against the measured time t taken for 1 ml of condensate to collect in tube B. The calibration points lie on a very good straight line, demonstrating the accuracy of the method.

Extrapolation of the line to $t = 0$ gives the correction R_0 to be applied in an absolute measurement of thermal resistance (R_0 takes account of contact resistances as well as heat losses).

It has already been mentioned that the upper vessel G is enclosed in a dewar flask to minimize heat losses. The sample must also, of course, be provided with heat insulation; a series of rings are available to surround the sample (two such rings can be seen at the right of the stand in fig. 2*a*). In order to carry out thermal conductivity measurements at temperatures very different from room temperature, both vessels and the sample must be surrounded by shields, held at the appropriate temperatures by baths in which the same liquids as in A and G are kept at the boil. For measurements below room temperature, where G and A thus contain liquids that are gaseous at room temperature, the vapour from G need not be condensed in a cooler but can be collected and measured in a gas meter.

As regards the liquids themselves, pairs can be found for the whole temperature range from −200 to +400 °C having suitable boiling points differing by 5 to 15 °C. If necessary, the same liquid can be used for both vessels, and the boiling point in vessel A raised slightly by a small and constant increase of pressure, controlled by a pressurestat.

The samples used for both calibration and measurement are cylindrical in form, ranging in diameter from 16 to 18 mm and in length from 0.5 to 30 mm, depending on the thermal conductivity of the material. Samples of material of high thermal conductivity (pure metals) can be made in the form of hollow cylinders, say 10 mm in length and with a wall thickness preferably not less than 1.5 mm.

Summary. The two ends of a cylindrical sample, about 18 mm in diameter and 0.5-30 mm in length, are kept at constant temperatures, by contact with two boiling liquids of suitable boiling points, viz. differing by about 10 °C. The *time* is measured in which a quantity of heat flows, in the steady state, through the sample. This quantity is fixed very simply by the evaporation of a fixed quantity of liquid at the "cold" end, collected as condensate. In practice, two calibrated samples are measured first and a calibration line is plotted from which the thermal resistance of subsequent samples can be found at a glance. It is then not necessary to know the exact boiling points of the two liquids, nor the absolute amount of evaporated liquid, nor its heat of vaporization. A measurement takes 5 to 15 minutes and the error is not more than ± 3%. With some additional equipment the method can also be used for measurements at other than room temperature, between −200 and +400 °C.

CHEMICAL FORMULATION OF RADIO-ISOTOPES

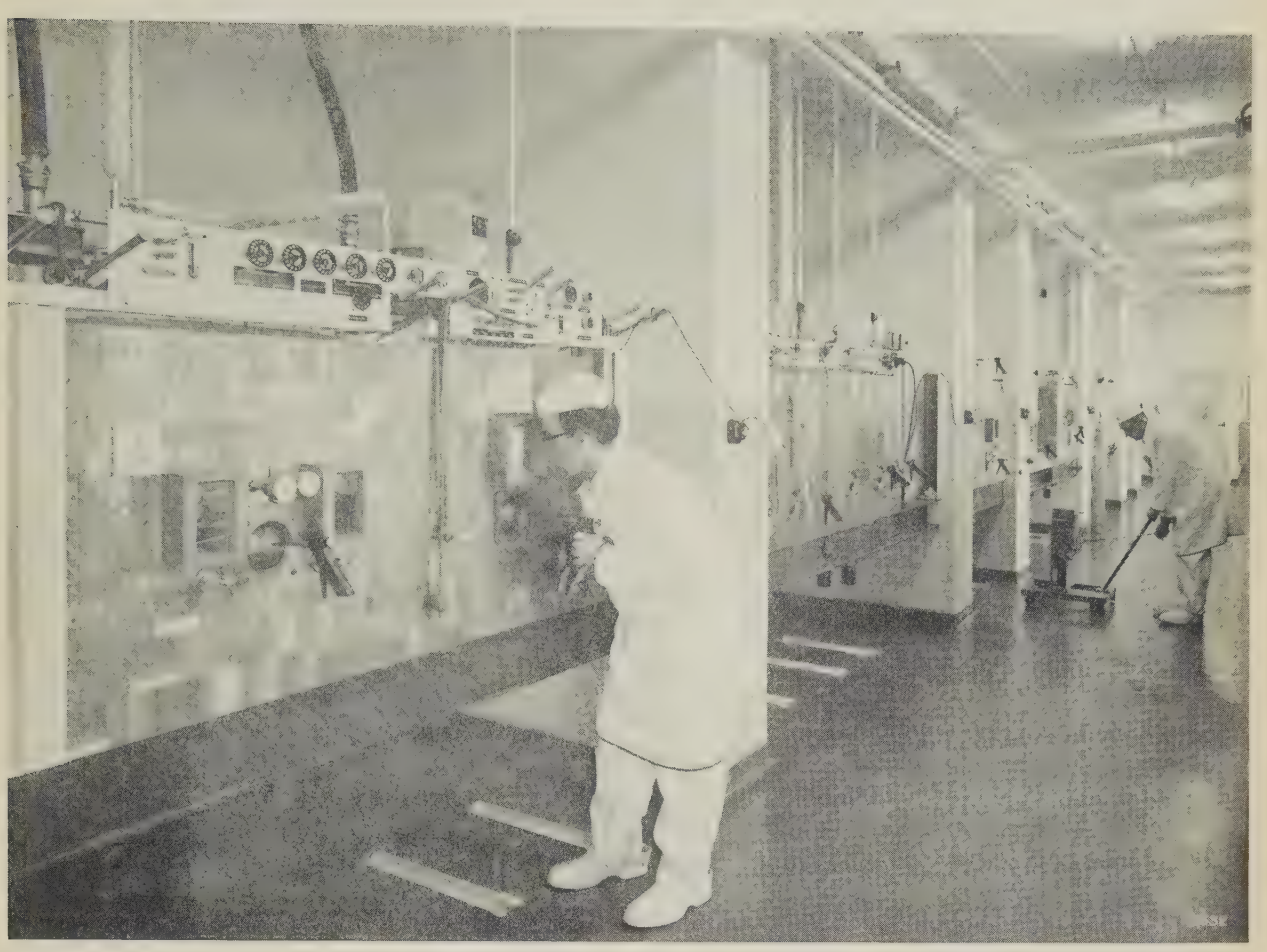

The photograph shows a part of the Isotope Laboratory of N.V. Philips Duphar in Amsterdam, where radio-isotopes produced in the Amsterdam cyclotron or in reactors at Kjeller (Norway), Mol (Belgium) or Saclay (France) are chemically processed. Among the isotopes handled are ^{131}I, ^{198}Au, ^{206}Bi, etc. Workers in the laboratory are protected from radiation hazards by performing all operations behind a thick lead wall, in fume cupboards with an underpressure of several cm water. The latter measure is to prevent contamination of the laboratory atmosphere by radioactive dust. A further safety measure is that all workers in the laboratory wear special clothing.

Manipulations of the radioactive substances are carried out with the aid of the usual remotely-controlled tongs. The man in the foreground is operating such a device. Windows of lead glass 20 cm thick make it possible to direct the tongs and follow the process. On the panel above the lead wall are cocks admitting water, steam, air, vacuum and certain standard reagents to the reaction vessel. Of the projecting rods on the panel, some serve for the opening and closing of the passage connecting one fume cupboard with the next, while others are for the operation of a balance for weighing the radioactive materials. The balance scale is visible on a ground-glass plate contained in the box seen just above the fume cupboard.

The fume cupboard at which the operator is busy is a pipetting cupboard, for transferring measured quantities of radioactive solutions. On the left of the operator are two rubber squeezers for sucking the solutions into the pipettes. In the cupboard on the left preparations for medical use can be sterilized. The two knobs between the two lead-glass windows open and close the autoclaves.

The fume cupboards are accessible only from underneath through special doors. The operator in the background is moving a transportable vessel containing the radioactive raw material to a position under the door of a fume cupboard. The guides in the floor ensure that the vessel is placed precisely under the door. The vessel is then raised until it just touches the door; the latter is opened from outside, whereupon the vessel is raised further into the cupboard. The contents may now be manipulated in the fume cupboard. The same procedure in the reverse order accomplishes removal of the vessel and closing of the door.

PERFORMANCE TESTS ON LOUDSPEAKERS

by M. T. HAITJEMA, W. KOPINGA and S. J. PORTE. 53.08:621.395.623.7

The article below describes a number of established methods of loudspeaker testing used over the years at Philips. These methods have proved particularly valuable in the design of loudspeakers and loudspeaker cabinets. Some are also well adapted for sampling inspection during manufacture.

The loudspeaker tests discussed in this article are concerned with:

a) the variation of sound pressure as a function of frequency,
b) the variation of loudspeaker impedance as a function of frequency,
c) the resonance frequency,
d) transients, such as occur when the signal applied to the loudspeaker suddenly drops to zero,
e) directivity patterns, giving the sound pressure in different directions at constant frequency in polar coordinates, and
f) the variation of loudspeaker efficiency as a function of frequency.

Sound pressure, impedance and efficiency are recorded as a function of frequency on a strip-chart recorder; the transients and the directivity patterns are displayed on a cathode-ray oscilloscope [1]).

Sound pressure as a function of frequency

The procedure for recording the variation of the sound pressure of a loudspeaker as a function of frequency (frequency response) is as follows. The signal from a signal generator is applied to the loudspeaker under test via an amplifier. Mounted in line with the axis of the loudspeaker [2]) is a condenser microphone, the signal from which is amplified and recorded. Loudspeaker and microphone are situated in an acoustically dead (non-reverberant) room at a distance of 50 cm apart (*fig. 1*). This distance proved to be the best compromise in connection with the imperfections of the dead room and the dimensions of the loudspeaker (provided that the diameter of the cone is not larger than about 30 cm).

A small motor drives a rotary capacitor in the signal generator such that the frequency is swept from 0 to 20000 c/s, the range from 0 to 100 c/s linearly with time and the range from 100 to 20000 c/s logarithmically (equal times for each swept octave). The same motor drives the strip-chart recorder. To allow for possible small discrepancies between the frequency scale printed on the paper strip and the true frequency variation, the generator signal is automatically interrupted for a moment as its frequency passes 1000 c/s.

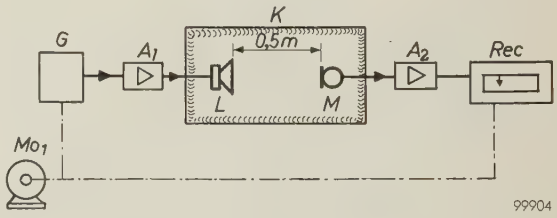

Fig. 1. Block diagram of apparatus for recording the sound pressure of a loudspeaker L as a function of the frequency of a signal generator G. A_1 amplifier with 50 W output stage in push-pull. M condenser microphone. A_2 microphone amplifier. *Rec* recorder. Mo_1 motor, which causes the frequency to sweep from 0 to 20000 c/s and also drives the strip-chart recorder. K dead room.

The amplifier A_1 between the signal generator and the loudspeaker has a 50 W output stage in push-pull fitted with four EL 34 pentodes in class AB. The output transformer is provided with taps for matching to loudspeaker coils of different impedance. Depending on whether the output current or output voltage is to be kept constant with varying frequency, 20-fold negative current or voltage feedback can be switched in. The frequency response is recorded at a constant current, viz. $\sqrt{50 \times 10^{-3}/R}$ amp, where R is the DC resistance of the loudspeaker coil in ohms. This means a power consumption of 50 mW at low frequencies.

The microphone amplifier A_2 is corrected so as to give the condenser microphone plus amplifier a flat frequency response from 20 to 20000 c/s.

The recorder is fitted in the usual way with an input potentiometer whose sliding contact is coupled with the stylus. The arrangement is such that the stylus is at rest only when the sliding contact is at

[1]) The methods of recording directivity patterns and efficiency curves were described briefly in T. Ned. Radiogenootschap **23**, 303-309, 1958 (No. 6).

[2]) All the tests described here were made on loudspeakers without baffles. Thus, the properties of the loudspeaker itself were measured, and not the additional properties of a baffle.

a point having a potential of 10 mV with respect to earth (the deflection is thus zero for input signals smaller than 10 mV). The relation between the deflection of the stylus and the input voltage depends on the resistance law of the potentiometer. In the present case a decibel scale is required for the ordinate of the response curve, whereas a linear scale is needed for the impedance characteristic, discussed below. Two interchangeable input potentiometers are therefore used, one of which gives a logarithmic and the other a linear scale, both for input voltages from 10 mV upwards.

Fig. 2 shows a loudspeaker frequency response curve recorded by the method described.

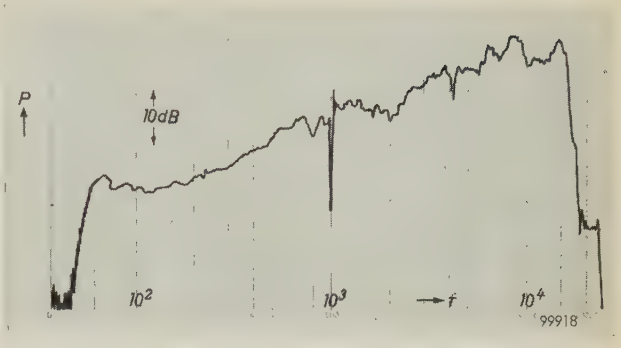

Fig. 2. Recording of sound pressure P as a function of frequency f (frequency response), obtained by the method illustrated in fig. 1. Sound-pressure scale logarithmic; frequency scale linear from 0 to 100 c/s, logarithmic from 100 to 20 000 c/s. At 1000 c/s there is a marker dip, obtained by momentarily interrupting the signal at this frequency.

Electrical impedance as a function of frequency

The electrical impedance of a loudspeaker is the ratio of the voltage across the loudspeaker coil to the current through it. When the current is kept constant, the voltage is thus proportional to the impedance. For recording the impedance/frequency curves the loudspeaker is again fed via the above-mentioned push-pull amplifier (with negative current feedback) with an audio signal from the signal generator, and the voltage across the loudspeaker coil is recorded. In this case the recorder uses the potentiometer giving a linear scale.

Fig. 3 shows two examples of impedance curves. Unlike curve *1*, curve *2* was recorded on a loudspeaker fitted with a short-circuiting ring [3]). This causes the impedance to rise much less sharply with frequency, thereby improving the reproduction of high notes.

Determination of the resonance frequency

The resonance frequency of a loudspeaker is the frequency at which the electrical impedance shows a maximum, by analogy with an inductance and capacitance in parallel which, in the region of the resonance frequency, form the electrical equivalent of the loudspeaker. The resonance frequency depends on the construction of the loudspeaker and also, where present, on the cabinet. The importance of the resonance frequency lies in the fact that it constitutes roughly the lower limit of the spectrum which the loudspeaker is capable of reproducing. (Below the resonance frequency the sound pressure drops with decreasing frequency by 18 dB per octave in the case of a loudspeaker without baffle, and by 12 dB per octave in the case of a loudspeaker in an infinitely large baffle.)

[3]) See Philips tech. Rev. **18**, 313, 1956/57.

The resonance frequency is determined by keeping the voltage across the loudspeaker constant (negative voltage feedback) and by adjusting the frequency of the signal generator until the current is minimum; this frequency is the resonance frequency. The constant voltage is chosen such that the minimum current is 50 mA for loudspeakers of low resistance (of the order of 10 ohms), and 5 mA for loudspeakers of high resistance (400 or 800 ohms) [4]). At these currents the amplitude of the cone is so small that non-linearity in the deformation of the centering ring or of the rim of the cone can be neglected.

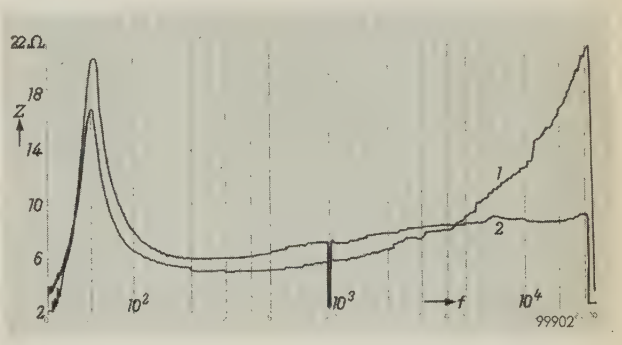

Fig. 3. Recordings of the impedance Z of a loudspeaker (linear scale) as a function of frequency f (in c/s). Curve *2* refers to a loudspeaker fitted with a short-circuiting ring [3]), curve 1 to a loudspeaker without such a ring. The flatter shape of curve *2* implies better reproduction of the high notes.

For determining the resonance frequency of loudspeakers in manufacture, an instrument giving a direct reading is preferred. An instrument of this kind has been devised, in which the loudspeaker under test functions as the *LC* circuit of an oscillator. The latter is provided with both positive and negative feedback. Both feedback circuits contain

[4]) For high-resistance loudspeakers, see Philips tech. Rev. **19**, 42, 1957/58.

non-linear elements which are dependent on the current. This makes the current through the loudspeaker virtually independent of the damping at resonance, the value of which may differ considerably for loudspeakers of different types. The frequency at which the system oscillates is the resonance frequency of the loudspeaker and can be read from a direct-reading frequency meter.

Oscilloscopic display of transients

Of great importance to the good reproduction of speech and music is the way in which the loudspeaker responds to plosives and the sudden entry of musical instruments, that is its response to abrupt initiation or removal of the electrical signal. The resultant transients, and in particular the subsidence transient following the interruption of the signal, can be studied by the following method.

The loudspeaker is supplied with a periodically interrupted sinusoidal signal (sine wave trains). The acoustic signal delivered by the loudspeaker, and picked up by a neighbouring microphone, is displayed on a cathode-ray oscilloscope. The oscillogram shows the initiation transient as well as the subsidence transient. The display of the latter can be improved by inserting a device between microphone and oscilloscope which suppresses the microphone signal for the duration of each applied wave train, so that only the transient proper remains visible. Loudspeaker and microphone must be set up in an acoustically dead room, as otherwise reverberation would appear as spurious deflections in the oscillogram.

Fig. 4 shows the block diagram of the circuit. An electronic switch E_1 between the signal generator G and the push-pull amplifier A_1 produces the sinusoidal signals by intermittently passing the voltage from the signal generator for a certain number of cycles n and blocking it for the same length of time; the signal is switched on and off at the moment the sine wave passes through zero. The electronic switch is controlled by a square-wave voltage supplied by the frequency-divider stages C (bistable multivibrators), one or more of which can be switched in to set n at 4, 8, 16 or 32 cycles. The first divider stage receives its input signal from the signal generator via the circuit B, which converts the sinusoidal signal into a square-wave voltage. *Fig. 5a* shows an oscillogram of the microphone signal for $f = 2500$ c/s, $n = 16$.

To suppress the microphone signal during each applied wave train, an electronic switch E_2 is placed between the microphone amplifier A_2 and the

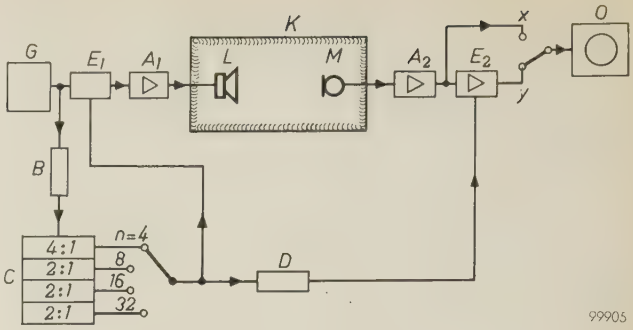

Fig. 4. Block diagram of the equipment for displaying transients. G signal generator. E_1 electronic switch producing wave trains from the sinusoidal voltage. A_1 push-pull amplifier. L loudspeaker under test and M microphone in dead room K. A_2 microphone amplifier. E_2 electronic switch for suppressing the microphone signal during the presence of the wave train. O cathode-ray oscilloscope. B circuit for converting the sinusoidal waveform into a square-wave form. C frequency dividers controlling electronic switches E_1 and E_2; they deliver square-wave forms of fundamental frequencies $^1/_4$, $^1/_8$, $^1/_{16}$ and $^1/_{32}$ times the frequency f of the signal generator. D device which delays the control signal for E_2 by an amount equal to the time taken by the sound to travel from L to M.

oscilloscope. This switch is controlled by the same square-wave voltage as E_1, but roughly in anti-phase and moreover with a fixed time-delay equal to the time which the sound from the loudspeaker takes to reach the microphone. The way in which the control signal is delayed is explained in *fig. 6*. The suppression is effective when the oscilloscope in fig. 4 is

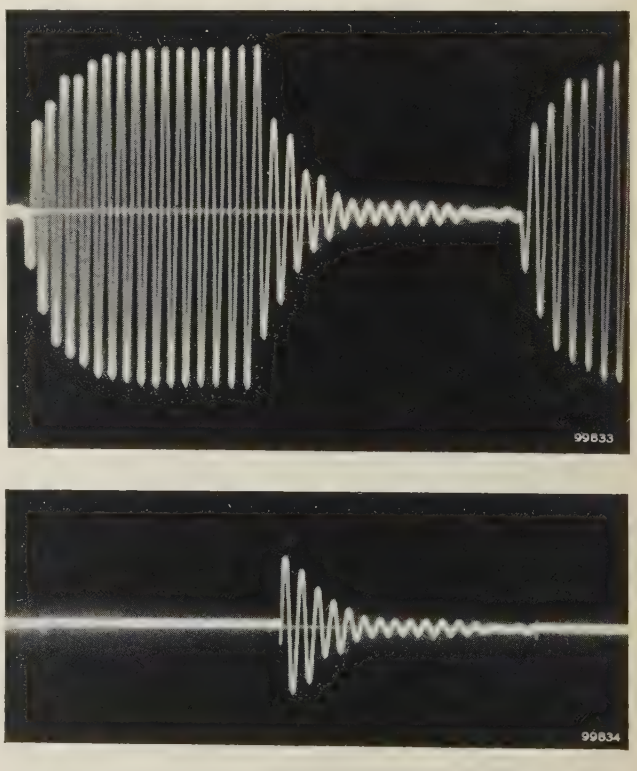

Fig. 5. *a*) Oscillogram of the microphone voltage in fig. 4 (oscilloscope connected to point x).
b) Oscilloscope connected to point y in fig. 4: the microphone signal is suppressed for the duration of the wave train itself, leaving only the transient visible.

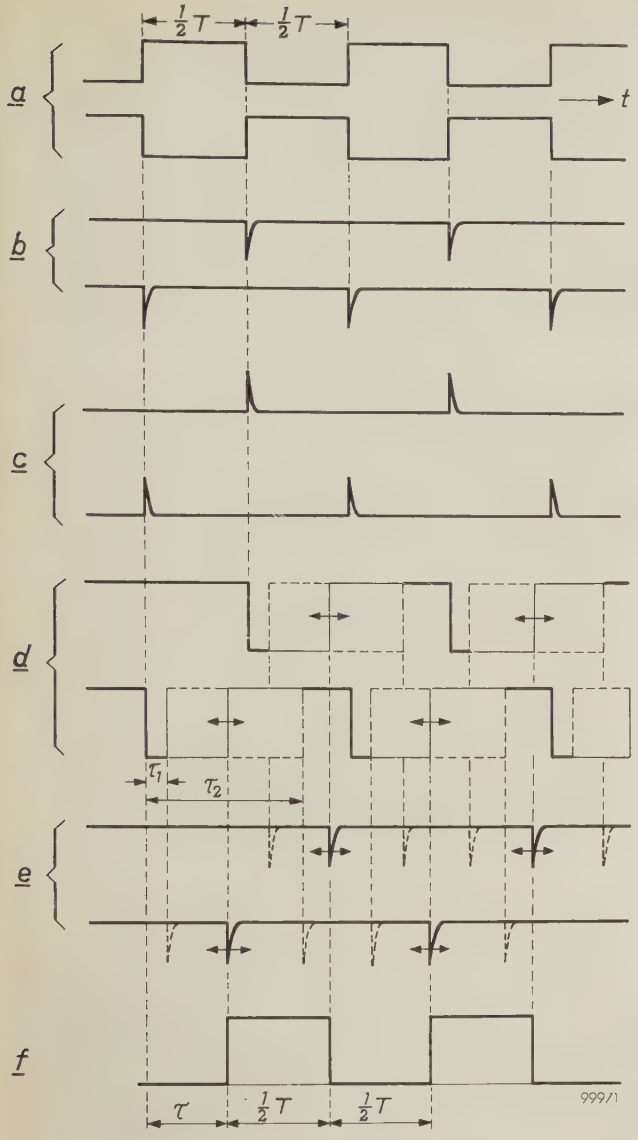

Fig. 6. Illustrating the way in which network D (fig. 4) delays the control signal for the electronic switch E_2 by a variable time τ, independent of the frequency f.
a) Square-wave voltages in anti-phase, derived from the frequency dividers C (fig. 4). A half period $\frac{1}{2}T$ comprises n cycles of the signal-generator voltage ($n = 4$, 8, 16 or 32).
b) Negative pulses obtained by differentiating the square-wave signals (*a*) and blocking the positive pulses.
c) Positive pulses obtained by amplifying the pulses in (*b*). The pulses (*c*) control a monostable flip-flop which, after each triggering pulse, returns to the quiescent state with an adjustable delay (by means of RC network with variable resistance).
d) Output of monostable flip-flop. The reset time of the flip-flop can be varied between the limits τ_1 and τ_2.
e) Pulses produced by differentiating, clipping and amplifying the signal in (*d*). These pulses can be varied in time between the limits τ_1 and τ_2, and are used to trigger a second multivibrator.
f) Square-wave voltage delivered by the second multivibrator. The signals in (*d*) are so adjusted that the square-wave voltage (*f*) has the same half period $\frac{1}{2}T$ as the signals in (*a*), but are displaced relative thereto by a variable interval τ. The signal (*f*) controls the electronic switch E_2 (fig. 4).

connected to point y. The resultant oscillogram of the transient alone is shown in fig. 5*b*.

As regards the transients at lower frequencies it makes a great difference whether the push-pull amplifier A_1 operates with negative current or voltage feedback. In the first case the amplifier behaves like a current source. Its internal resistance — in parallel with the loudspeaker — is then about 100 × higher than the loudspeaker resistance: the loudspeaker is thus only feebly damped and the transient takes a relatively long time to subside. With negative voltage feedback the amplifier behaves like a voltage source, the internal resistance is low (about 0.1 ohm): the loudspeaker is then strongly damped and therefore the transient is short-lived. The difference can be seen in the oscillograms in *fig. 7a* and *b*.

Some particulars of the oscilloscope are discussed at the end of the following section.

Display of directivity patterns

The directivity pattern of a loudspeaker presents the variation of the sound pressure — at a given distance and at constant frequency — in different directions. The form of the pattern depends on the frequency and on the dimensions and construction of the loudspeaker and of the cabinet or baffle, if present.

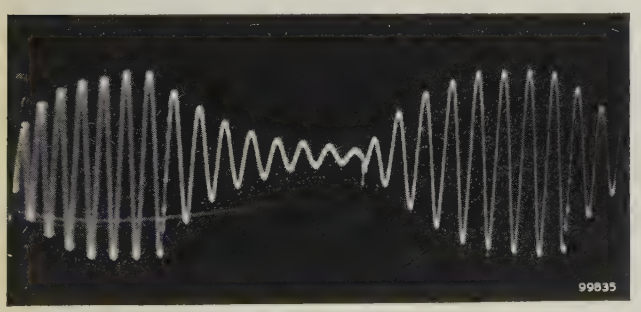

a

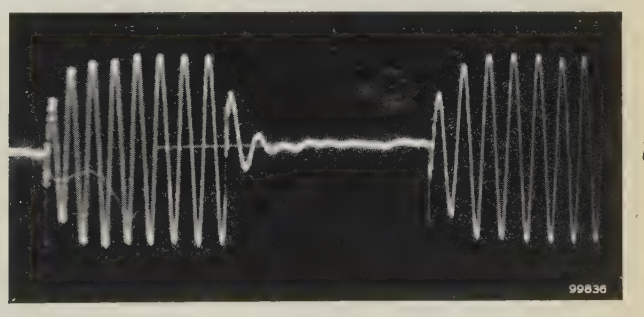

b

Fig. 7. Oscillograms of the microphone voltage (oscilloscope in fig. 4 connected to point x) at $f = 180$ c/s, $n = 8$. In (*a*) the amplifier A_1 operated with negative current feedback so that the loudspeaker was only weakly damped; in (*b*), the amplifier operated with negative voltage feedback so that the loudspeaker was heavily damped.

In our test set-up the loudspeaker is rotated in front of a fixed microphone in an acoustically dead room (*fig. 8*). By a method presently to be discussed, the logarithmically-amplified microphone signal is displayed on an oscilloscope in polar coordinates as a function of direction and at constant frequency.

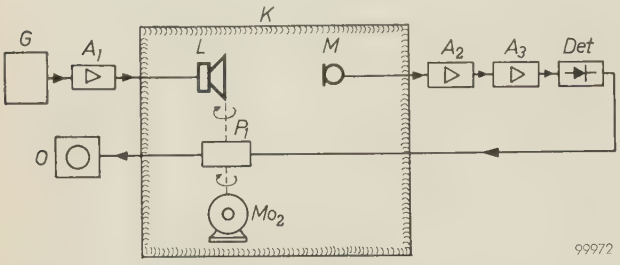

Fig. 8. Set-up for obtaining directivity patterns. *G* signal generator. A_1 push-pull amplifier. *L* loudspeaker under test in dead room *K* and, together with the liquid potentiometer P_1, rotated about a vertical axis by motor Mo_2. *M* microphone. A_2 microphone amplifier. A_3 logarithmic amplifier. *Det* detector. *O* oscilloscope.

We shall first explain how a polar diagram can be presented on an ordinary oscilloscope with two pairs of deflection plates. When a voltage $E \sin \omega t$ is applied to one pair of plates and a voltage $E \cos \omega t$ to the other pair, a circle is traced on the screen [5]). If these voltages are modulated in amplitude by a periodic time-function of fundamental frequency $k.\ \omega/2\pi$ (k an integer), a "modulated circle" is produced, that is to say one in which the radius is varied. The angle ωt is kept constantly equal to the angle α through which the loudspeaker is rotated during the time interval from 0 to t, and the amplitudes E are modulated in accordance with the logarithmically amplified microphone signal.

[5]) It is assumed for the sake of simplicity that the two pairs of plates are equally sensitive. The difference in sensitivity that actually exists must be corrected by adjusting the amplitudes of the two voltages to the correct ratio.

The voltages $E \sin \omega t$ and $E \cos \omega t$ are taken from a liquid potentiometer, the principle of which is illustrated in *fig. 9*. An insulating container *1* is filled with a conductive liquid (ethylene glycol). On opposite sides of the container carbon plates (*2*, *3*) are mounted, and between them a disc *4* of insulating material is rotated at a constant angular velocity ω. Fitted to the periphery of the disc, 90° apart, are two contacts of graphite (*5*, *6*) which are led out via slip rings. Connected between plates *2* and *3* is a centre-tapped battery of voltage $2E$, the centre-tap being earthed. The liquid in the plane of symmetry between the plates is therefore at earth potential, and the voltages on *5* and *6* vary, with respect to earth, as $E \sin \omega t$ and $E \cos \omega t$, respectively (disregarding a constant factor equal to the ratio of the diameter of the disc to the distance between the carbon plates).

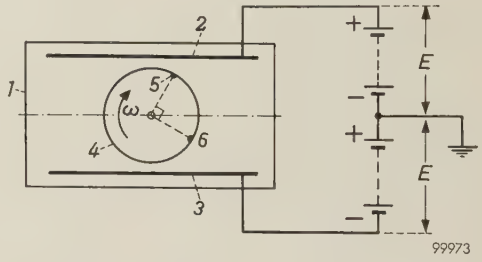

Fig. 9. Liquid potentiometer (P_1 in fig. 8) seen from above. *1* insulating container filled with a conducting fluid. *2*, *3* carbon plates. *4* disc of insulating material, rotating with angular velocity ω. *5*, *6* graphite contacts 90° apart on the periphery of the disc *4*. When voltages $+E$ and $-E$ with respect to earth are applied to plates *2* and *3*, the potentials of contacts *5* and *6* vary according to $E \sin \omega t$ and $E \cos \omega t$, respectively.

When these two voltages are applied to the deflection plates of the oscilloscope, a circle is traced on the screen which, when the applied voltage $2E$ is varied, becomes a "modulated circle". This varying DC voltage is obtained by rectifying the

1000 c/s

2000 c/s

3000 c/s

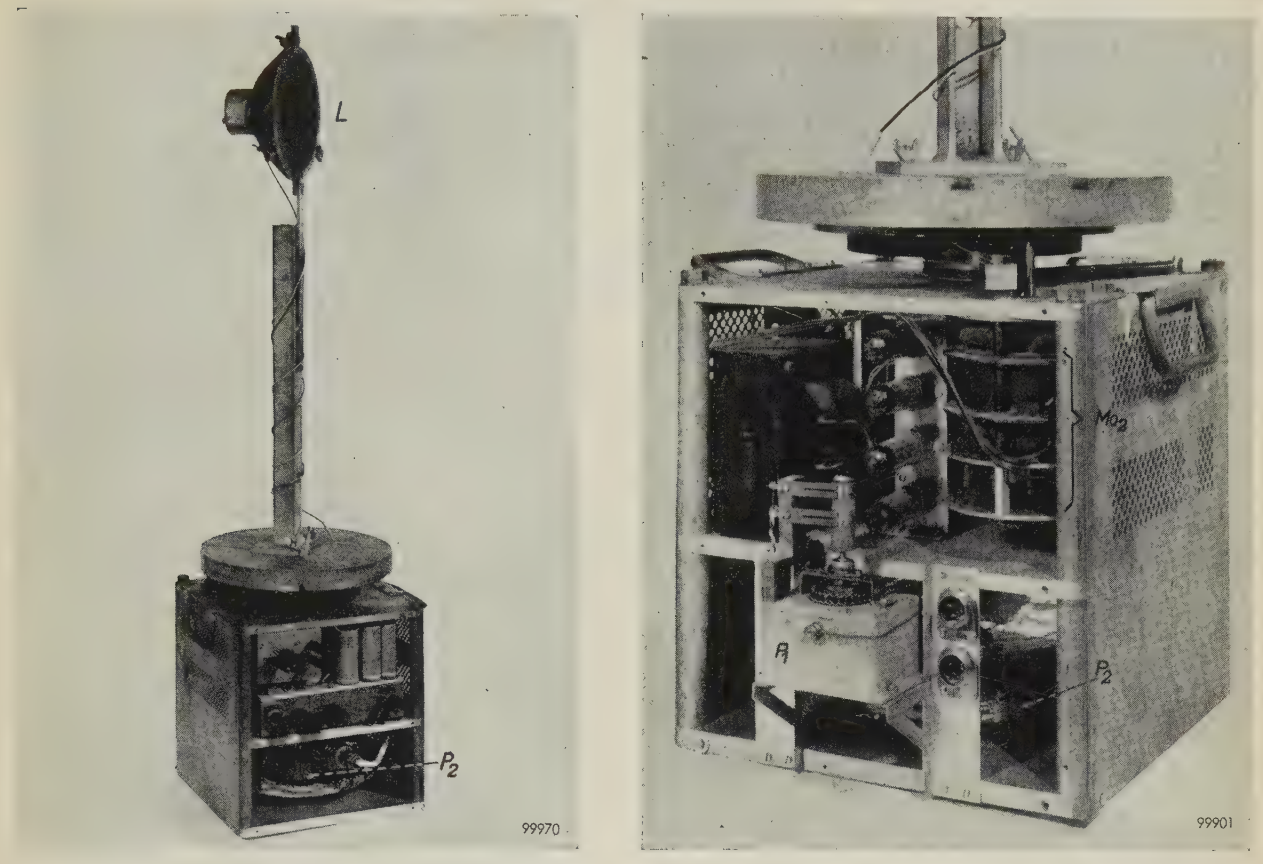

a *b*

Fig. 10. *a*) Mechanism for rotating the loudspeaker L about a vertical axis ($^1/_3$ rev per sec for recording directivity patterns). P_2 potentiometer required for recording efficiency curves. *b*) Mechanism seen from the other side, revealing the liquid potentiometer P_1 (cf. figs. 8 and 9) and the driving motor Mo_2.

output voltage of the logarithmic amplifier A_3 (fig. 8) by the detector *Det.*

The rotary mechanism, with a loudspeaker mounted on it, is shown in *fig. 10a.* The liquid potentiometer (P_1) can be seen in fig. 10*b*. *Fig. 11* reproduces some examples of directivity patterns recorded with the set-up described.

The logarithmic gain is obtained by using type EBF 80 pentodes in the first two stages of A_3. A feature of this valve is that the logarithm of the transconductance S at constant screen-grid voltage is approximately a linear function of the control-grid voltage (*fig. 12*). The rectified output signal is used for negatively biasing both EBF 80 pentodes. As a result, the logarithm of the gain is virtually proportional to the amplitude of the input signal, so that the microphone signal is recorded on

8000 c/s

16 000 c/s

Fig. 11. Directivity patterns recorded at different frequencies on a double-cone loudspeaker, type 9710 M (outer diameter 216 mm), without cabinet or baffle.

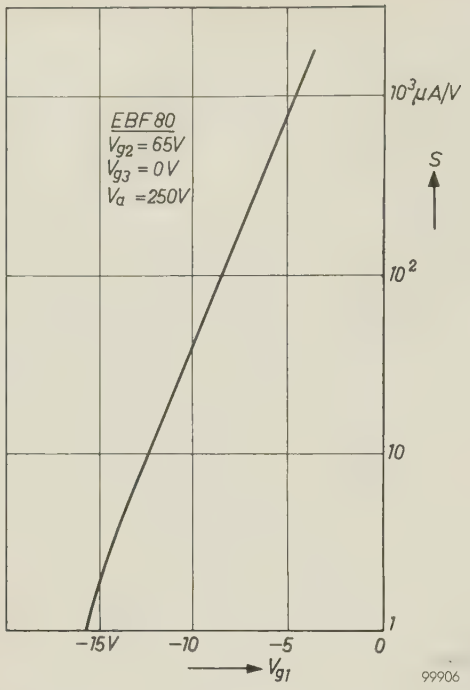

Fig. 12. Transconductance S (on logarithmic scale) of a pentode type EBF 80 as a function of control-grid voltage V_{g1}, at a screen-grid voltage of 65 V, a suppressor-grid potential of zero volts and an anode potential of 250 V. The characteristic is approximately straight, so that S is virtually a logarithmic function of V_{g1}.

a logarithmic scale.

The detector *Det* consists of two full-wave rectifiers, the output from one being positive and from the other negative with respect to earth. Full-wave rectifiers are used to reduce ripple and to provide effective smoothing. The ripple voltage must be kept small because it is superimposed as a spurious effect on the modulation of the circle. On the other hand, there is a limit imposed on the time constant for the smoothing: if it is too long, the direct voltages cannot vary rapidly enough and the pattern loses detail. The maximum permissible time constant is determined by the speed at which the loudspeaker is rotated (here $^1/_3$ revolution per second) and by the smallest angle of rotation within which the maximum pressure difference in the pattern must still be reasonably perceptible. This angle was taken as 5°, and the maximum permissible time constant is therefore: $(^5/_{360}) \times 3 = {}^1/_{24}$ sec. With full-wave rectification adequate smoothing is obtained with this fairly short time constant.

The oscilloscope

The transients and the directivity patterns are displayed on two oscilloscope tubes connected in parallel. One of these serves as the oscilloscope proper and must have a very long persistence screen, the time taken to trace a directivity pattern being 3 sec. The other tube is used for photographing oscillograms and is accordingly provided with a blue-luminescent phosphor of short persistence. Focusing and brilliance for the two tubes are controlled separately. A photograph of the oscilloscope rack appears in *fig. 13*.

For the recording of directivity patterns, both components of the signal voltage are modulated with the loudspeaker rotational frequency of $\frac{1}{3}$ c/s. AC amplifiers would have to be given impractically large RC values in order to reproduce such low-frequency signals without distortion. DC amplifiers are therefore used, the principal data for which are as follows:

Gain . . . . . 2000 ×,
± 1 dB from 0 to 20 kc/s,
± 3 dB to 50 kc/s.
Max. output voltage . 60 V.
Distortion . . . . . < 2%.
Input impedance . . . approx. 0.5 MΩ.

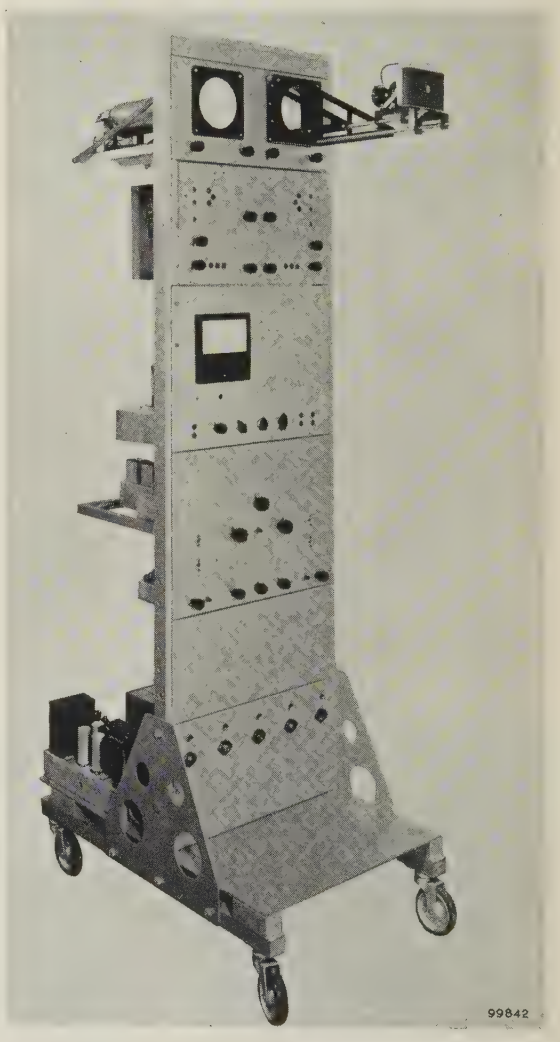

Fig. 13. Rack with two oscilloscope tubes and associated equipment. The left tube serves for observation of the directivity patterns and has a greenish-yellow luminescent phosphor of long persistence. The right tube is used when oscillograms are to be photographed, and has a blue-luminescent screen of short persistence.

The study of transients calls for a sawtooth sweep voltage of very low frequency, in order to be able to display at least one complete wave train plus the interval between two trains. The time involved may be up to 64 cycles of the audio frequency used. At the lowest audio frequency (20 c/s) the lowest sweep frequency must therefore be $^{20}/_{64} \approx 0.3$ c/s. The time-base generator uses a Miller integrator based on a transitron circuit [6]). This produces a closely linear sawtooth voltage of very low frequency without the need for a high supply voltage or high capacitances. The sawtooth voltage is amplified by one of the DC amplifiers mentioned above.

Loudspeaker efficiency as a function of frequency

The efficiency η of a loudspeaker is the ratio of the radiated acoustic power W_0 to the electrical input power W_i. The latter is the sum of W_0 and the losses, such as the electrical loss I^2R in the coil and the mechanical losses in the centering ring and in the rim of the cone. In the region of 500 c/s the efficiency of most loudspeakers is only a few per cent [7]); the losses there are thus much greater than W_0, and by far the largest part of these losses is due to I^2R. It is therefore the usual practice to measure efficiency at constant current I, and to regard W_i to the first approximation as identical with I^2R, although this is not correct in three respects:

1) it neglects the other losses with respect to I^2R,
2) it neglects W_0 with respect to I^2R,
3) it takes no account of the fact that R is frequency-dependent.

These errors only become significant, however, at frequencies higher than about 1000 c/s, mainly because the iron losses (or the copper losses if the loudspeaker is fitted with a short-circuiting ring) are then no longer negligible in relation to I^2R. At these frequencies, then, it is necessary to apply to the recorded curve a correction as a function of frequency. This correction takes account of the extra losses and also, in the region of several kc/s, of the radiated power. We shall not discuss here the determination of the correction curve, which can be done by the so-called three-voltmeter method.

Let us now turn to the method of determining the radiated acoustical power W_0. We assume that the loudspeaker possesses rotational symmetry about its axis. The sound intensity at a distance r from the loudspeaker, and in a direction α with respect to the axis, will be denoted by $I(\alpha)$. The power $\mathrm{d}W_0$ radiated between the directions α and $\alpha + \mathrm{d}\alpha$ (see *fig. 14*) is then:

$$\mathrm{d}W_0 = I(\alpha) \times 2\pi r \sin\alpha \times r\, \mathrm{d}\alpha .$$

For $I(\alpha)$ we can write $P^2(\alpha)/\varrho c$, where $P(\alpha)$ is the r.m.s. sound pressure at a distance r in a direction α, ϱ is the density of the air and c is the velocity of sound in air. This gives us:

$$\mathrm{d}W_0 = \frac{2\pi r^2}{\varrho c} P^2(\alpha) \sin\alpha\, \mathrm{d}\alpha .$$

The total radiated power W_0 is therefore:

$$W_0 = \frac{2\pi r^2}{\varrho c} \int_0^{\pi} P^2(\alpha) \sin\alpha\, \mathrm{d}\alpha . \quad . \; . \quad (1)$$

If we have the directivity pattern of the loudspeaker at various frequencies, we could derive W_0 at these frequencies from the bounded area of the curve obtained by multiplying the radius vectors in

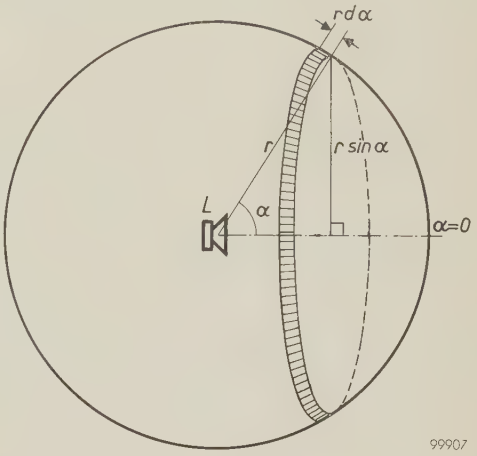

Fig. 14. When the loudspeaker L possesses rotational symmetry about the axis $\alpha = 0$, a sound intensity $I(\alpha)$ prevails at every point of the hatched segment. The surface area of the segment is $(2\pi r \sin\alpha) \times r\, \mathrm{d}\alpha$. The acoustic power incident on the segment is $I(\alpha) \times 2\pi r^2 \sin\alpha\, \mathrm{d}\alpha$. By integrating this expression over α (see eq. 1), we find the total radiated acoustic power W_0.

the directivity pattern by $\sqrt{|\sin\alpha|}$. This area can be found by planimetry, but this is a cumbersome method, particularly if it is required to find the efficiency for a whole series of frequencies.

In principal it would be possible to measure W_0 by disposing a very large number of microphones in a circle around the loudspeaker; by squaring the microphone voltages, multiplying them by the corresponding value of $|\sin\alpha|$ and adding the results together, we should find the approximate value of the integral in (1). However, this method is ruled out too by the high costs of the numerous condenser microphones that would be needed.

Fig. 15 illustrates a method by which, with only one microphone, the loudspeaker efficiency can be recorded directly as a function of frequency. The microphone is set up in a dead room, and in front

[6]) See e.g. F. Kerkhof and W. Werner, Television, Philips Technical Library, 1952, page 138 *et seq.*

[7]) J. de Boer, The efficiency of loudspeakers, Philips tech. Rev. **4**, 301-307, 1939.

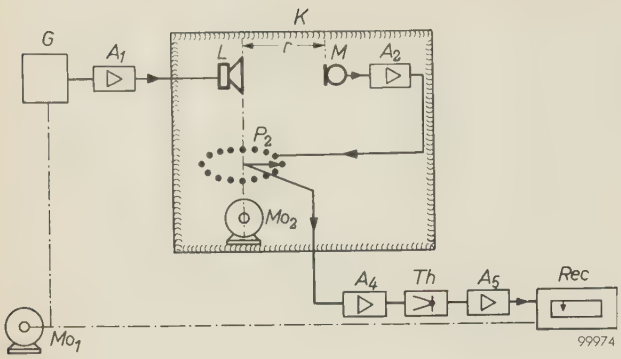

Fig. 15. Set-up for recording the efficiency of a loudspeaker as a function of frequency. L loudspeaker under test, fed from signal generator G via push-pull amplifier A_1. K dead room. M microphone. A_2 microphone amplifier. P_2 rotary potentiometer whose arm, like the loudspeaker, is rotated by the motor Mo_2 at about 3 revs/sec; the potentiometer has a $\sqrt{|\sin \alpha|}$ law. A_4 amplifier. Th thermocouple. A_5 DC amplifier. Rec recorder. The motor Mo_1 causes the frequency f of the signal generator to traverse the whole audio range in about 5 minutes, and at the same time drives the strip recorder at a corresponding rate.

of it the loudspeaker is rotated uniformly about a vertical axis. The angle α between the geometrical axis of the loudspeaker and the fixed connecting line between loudspeaker and microphone thus passes periodically through all values from 0 to 2π. To the output of the microphone amplifier a potentiometer P_2 is connected, whose arm rotates together with the loudspeaker. The potentiometer is so wound as to give a $\sqrt{|\sin \alpha|}$ law. The design of this potentiometer, which must be entirely free from crackle, is illustrated in *fig. 16*; see also fig. 10*a* and *b*. The output voltage of the potentiometer is applied to an amplifier which feeds the heater of a vacuum thermocouple. The direct voltage delivered by the thermocouple is amplified and recorded on a strip-chart recorder. The movement of the paper is coupled with the rotation of the capacitor in the signal generator which feeds the loudspeaker (just as in the case of the frequency response, see above). The amplifier between the signal generator and the loudspeaker operates in this case with negative current feedback, so that the current through the loudspeaker remains just about constant throughout the frequency range swept.

The fact that the deflection of the recording stylus is proportional to the radiated power, so that the efficiency is directly recorded as a function of frequency, can be explained roughly as follows. The proportionalities involved are:

Microphone voltage . . . . . $\propto P(\alpha)$,
Input voltage, potentiometer . . $\propto P(\alpha)$,
Output voltage, potentiometer . . $\propto P(\alpha)\sqrt{|\sin \alpha|}$,
Alternating current, thermocouple $\propto P(\alpha)\sqrt{|\sin \alpha|}$,
Direct voltage, thermocouple . . $\propto P^2(\alpha)|\sin \alpha|$.

$P^2(\alpha) \sin \alpha$ appears in (1) under the integral sign. The integration over α from 0 to π is effected by the rotation of the loudspeaker. The thermal inertia of the thermocouple ensures that the direct voltage obtained is proportional to the mean square value

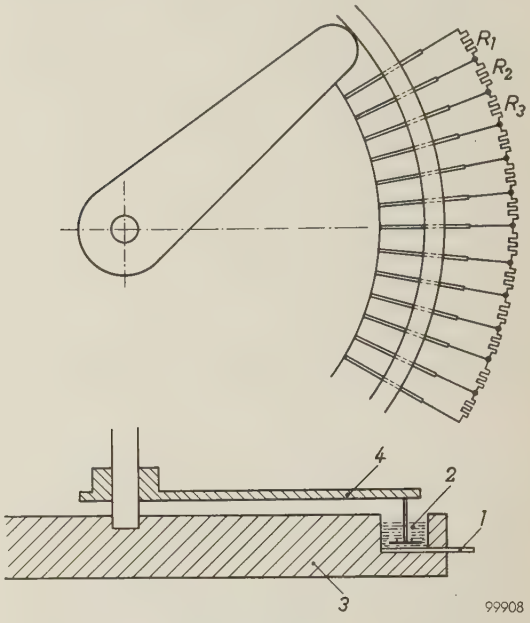

Fig. 16. Construction of the rotary potentiometer P_2 (fig. 15). $R_1, R_2, \ldots$ fixed resistors with values giving the potentiometer a $\sqrt{|\sin \alpha|}$ law. The taps are formed by 72 strip contacts *1* which are secured in the insulating plate *3* along the annular groove *2*. The groove is filled with a conducting liquid (ethylene glycol). The rotary arm *4* is clear of the strips but makes electrical contact with them via the conducting liquid. This construction guarantees complete freedom from crackle. The resistance values R are chosen low enough to make the conduction between the successive strips via the liquid negligibly low compared with the conduction through R. The fairly high contact resistance between the arm and the strips is of no consequence in that no current is drawn.

of the alternating current, which varies with α. A further condition is that the frequency should not change much during a single revolution of the loudspeaker. *Fig. 17* gives an example of an efficiency curve, which took about 5 minutes to record.

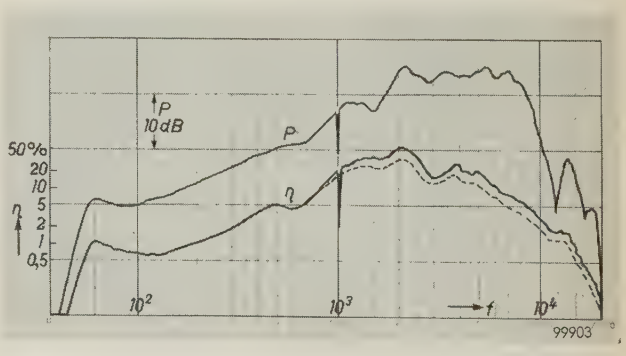

Fig. 17. Efficiency η (on logarithmic scale) recorded with the set-up in fig. 15; dashed curve: after correction for other losses than I^2R and for the radiated power. The recording was made in 5 minutes. For comparison, the frequency response (P) of the same loudspeaker is also shown.

When the loudspeaker is rotated through an angle α with respect to the position of the microphone, the instantaneous value $p(\alpha)$ of the sound pressure near the microphone is

$$p(\alpha) = P(\alpha)\sqrt{2}\sin(2\pi ft + \varphi),$$

where f is the sound frequency and φ is a phase angle.

Let the sensitivity of the microphone, including the microphone amplifier A_2, be s. The output voltage v_2 of A_2 is then:

$$v_2 = s\,P(\alpha)\sqrt{2}\sin(2\pi ft + \varphi).$$

The rotating potentiometer introduces a factor $\sqrt{|\sin\alpha|}$. Its output voltage, v_p, is therefore:

$$v_p = s\,P(\alpha)\sqrt{2\,|\sin\alpha|}\sin(2\pi ft + \varphi).$$

The thermocouple produces a direct voltage E_{th} which is proportional to the mean square value of v_p over half a revolution. Let the proportionality factor be ϑ, then:

$$E_{th} = \frac{\vartheta}{\pi}\int_0^{\pi} v_p^2\,d\alpha = \frac{2\vartheta s^2}{\pi}\int_0^{\pi} P^2(\alpha)\sin\alpha\sin^2(2\pi ft+\varphi)\,d\alpha. \quad (2)$$

Now we have

$$\sin^2(2\pi ft + \varphi) = \frac{1 - \cos 2(2\pi ft + \varphi)}{2}.$$

Hence (2) becomes:

$$E_{th} = \frac{\vartheta s^2}{\pi}\int_0^{\pi} P^2(\alpha)\sin\alpha\,d\alpha - \frac{\vartheta s^2}{\pi}\int_0^{\pi} P^2(\alpha)\sin\alpha\cos 2(2\pi ft+\varphi)\,d\alpha.$$

It is easy to see that the second integral will be approximately zero, for even the lowest audio frequency f (20 c/s) is still high compared with the number of revolutions made by the loudspeaker per second, viz. 3. This means that during half a revolution ($\alpha = 0 \rightarrow \pi$) the factor $\cos 2(2\pi ft + \varphi)$ swings to and fro many times between +1 and −1, thereby making this integral virtually zero. This also applies if f is gradually raised during half a revolution. To a good approximation, then, only the first integral remains:

$$E_{th} \approx \frac{\vartheta s^2}{\pi}\int_0^{\pi} P^2(\alpha)\sin\alpha\,d\alpha.$$

In conjunction with (1) this gives:

$$W_o \approx \frac{2\pi r^2}{\varrho c}\frac{\pi}{\vartheta s^2}E_{th} = \frac{2\pi^2 r^2}{\varrho c\vartheta s^2}E_{th},$$

which demonstrates the approximate proportionality between W_o and E_{th}.

We have tacitly assumed above that the wave front is spherical. If it is not spherical, the contribution of the second integral in (2) will, in general, not be so small. It can be calculated, however, for a dipole — and as such we can regard a loudspeaker at low frequencies — which turns at two revolutions pers econd, that at $f = 80$ c/s the contribution of the second integral is smaller than 1%.

Other methods of measuring W_o

Two other methods of measuring W_o may be briefly mentioned. One resembles the measurement of the luminous flux of a light source in an integrating photometer: loudspeaker and microphone are placed in an acoustically "hard" room (with reflecting walls) in such a way that the direct radiation from the loudspeaker to the microphone is negligible. Since the wavelengths of the sound are relatively long, fairly complicated measures are necessary to prevent the formation of standing waves and to bring about a sufficiently diffuse distribution of the sound. This subject has already been dealt with in this review [8]).

The other method of measuring W_o was devised by the British Broadcasting Corporation [9]). As in our case, a potentiometer is made to rotate together with the loudspeaker, but the potentiometer law here is $|\sin\alpha|$. Use is further made of a somewhat modified kilowatt-hour meter. To the current coil of this meter a current is applied which is proportional to the microphone voltage, hence to $P(\alpha)$; to the voltage coil a voltage is applied which is taken from the potentiometer and is proportional to $P(\alpha)\,|\sin\alpha|$. In accordance with the principle of the kilowatt-hour meter the number of revs per sec of the disc in this meter is thus proportional to $P^2(\alpha)\,|\sin\alpha|$. The integration over α from 0 to π is again effected by rotating the loudspeaker. Since the kilowatt-hour meter only works reliably at frequencies of about 50 c/s, the microphone voltage must first be detected and the resultant direct voltage converted into an alternating voltage of 50 c/s. The method is not suitable for recording.

Calibration

It only remains to describe how the scale of the recorder is calibrated in milliwatts.

The microphone is disconnected from the amplifier A_2 (fig. 15) and the input of A_2 is connected to a signal generator with an output millivoltmeter. With the potentiometer P_2 rotating we can now determine the proportionality factor β between the square of the input voltage V_i of A_2 and the deflection x of the recorder:

$$x = \beta V_i^2. \quad (3)$$

The sensitivity s_m of the microphone is known, i.e. the proportionality factor between the sound pressure P and the voltage V_i:

$$V_i = s_m P. \quad (4)$$

All that we need now is the relation between the sound pressure P and the power W_o radiated by the loudspeaker. This relation can be calculated for a point sound source. Let the radiated power from this point source be W_o (uniformly distributed in all directions), then at a distance r from the source the sound intensity is $I = W_o/4\pi r^2$, and the relation between sound pressure P and I at that distance is given by $I = P^2/\varrho c$. Hence:

$$P^2 = \frac{\varrho c}{4\pi r^2}W_o. \quad (5)$$

---

[8]) R. Vermeulen, The testing of loudspeakers, Philips tech. Rev. **4**, 354-363, 1939, in particular page 361.

[9]) A. Gee and D. E. L. Shorter, An automatic integrator for determining the mean spherical response of loudspeakers and microphones, B.B.C. Engng. Div. Monogr. No. 8, Aug. 1956.

From (3), (4) and (5) we find:

$$W_0 = \frac{4\pi r^2}{\varrho c\, s_m{}^2 \beta} x. \quad \ldots\ldots \quad (6)$$

In (6) the following are known:

r = distance from loudspeaker to microphone,
ϱ = density of the air (1.2 kg/m³ at 1 atm pressure and 22 °C),
c = velocity of sound (345 m/s at 22 °C),
s_m = sensitivity of the microphone, and
β = measured ratio between x and V_i^2.

With these known quantities we can therefore calculate the proportionality factor between W_0 and x.

In conclusion it may be noted that the equipment described can also be used *mutatis mutandis* for similar measurements on objects other than loudspeakers. Without any fundamental modifications it can serve, for example, for recording the frequency response and transients of amplifiers, and the directivity patterns of microphones, light sources and short-wave aerials.

Summary. Methods of testing loudspeakers are described, in which the sound pressure, the electrical impedance and the efficiency are recorded as a function of frequency (20-20 000 c/s) on a strip-chart recorder, whilst the directivity patterns at different frequencies and the transients produced by the sudden interruption of the electrical signal are displayed on a cathode-ray oscilloscope. The resonance frequency of the loudspeaker can also be determined. For most of the tests the loudspeaker and microphone (condenser type) are set up in an acoustically dead room. For recording the directivity patterns and the efficiency curve the loudspeaker is rotated about a vertical axis. About 5 minutes are required to record the efficiency curve.

ABSTRACTS OF RECENT SCIENTIFIC PUBLICATIONS BY THE STAFF OF N.V. PHILIPS' GLOEILAMPENFABRIEKEN

Reprints of these papers not marked with an asterisk * can be obtained free of charge upon application to Philips Electrical Ltd., Century House, Shaftesbury Avenue, London W.C. 2, where a limited number of reprints are available for distribution.

2723: K. van Duuren and G. J. Sizoo: The gas-discharge mechanism for the argon-alcohol proportional counter (Appl. sci. Res. **B 7**, 379-399, 1959, No. 5).

Accurate measurements of the gas multiplication factor were done for a number of proportional counters with various wire diameters ranging from 0.003 to 0.1 cm and for various gas pressures ranging from 67 to 220 mm Hg. From these results the ionization coefficient for the argon-alcohol gas mixture 9 : 1 was deduced. It appeared that in a few cases the equilibrium between the mean electron energy and the electrical field was slightly disturbed and the conditions for the non-equilibrium situation could be established from the experiments. Rose's and Korff's calculations of the gas multiplication factor in proportional counters were compared with the authors' experimental results, whereby rather large discrepancies were found. Comparison of the authors' experimental values of the ionization coefficient for argon-alcohol with the earlier published values for pure argon and alcohol gives and insight in the mechanism of the electron multiplication process in the argon-alcohol gas mixture 9 : 1.

2724: J. M. Stevels and A. Kats: Défauts de réseau dans le quartz cristallin et la silice fondue (Compte-rendu XXXIe Congrès int. Chim. industr., Liège, Sept. 1958, Vol. II, pp. 125-128, Mercurius, Antwerp). (Lattice defects in quartz and fused silica; in French.)

In the Si-O lattice of quartz and of fused silica, defects — either foreign atoms or vacancies — are almost always present. The former are often not detectable by classical chemical methods owing to their low concentration. By study of dielectric losses, absorption spectra and paramagnetic resonance it is possible to gain information on the chemical nature of these imperfections.

2725: K. van Duuren and J. Hermsen: Improved design for halogen-quenched end-window Geiger counters (Rev. sci. Instr. **30**, 367-368, 1959, No. 5).

Note reporting certain improvements in the design of end-window Geiger-Muller tubes. The improvements are concerned with modifying the electric field especially near the window, and consist of the use of a conducting window and of a spherical or hemispherical anode.

2726: N. W. H. Addink and L. J. P. Frank: Remarks apropos of analysis of trace elements in human tissues (Cancer **12**, 544-551, 1959, No. 3).

It is shown that unless neoplasms develop in tissues relatively rich in zinc, the zinc level of both serum and whole blood in carcinoma cases is subnormal. There is no connection between the zinc level of whole blood on the one hand and the iron (in hemoglobin) or water level on the other. Control of 3 groups of carcinoma patients by measuring the zinc content of their whole blood during the years 1955 to 1957 resulted in agreement between the physician's view and that of the laboratory studying zinc level alterations, in 80 to 90% of the cases. The authors' conclusions are: (1) Blood from cancerous patients generally shows a subnormal zinc level (with a mean value of 4.5 parts per million as compared to a value of 6.5 parts per million for blood from healthy subjects). Favourable progress against the disease is accompanied by an increase towards normal values. In the case of unfavourable progress, the low zinc level is persistent or it decreases still further. (2) In cases of tumor development in tissues relatively rich in zinc (the aberrant tumor groups), the zinc level has been found to be supernormal. A fall to the normal zinc level indicates favourable progress, whereas a permanent supernormal level indicates unfavourable development in the illness. Shortly before death, supernormal as well as subnormal values can be found.

2727: J. Hornstra: Models of grain boundaries in the diamond lattice, I. Tilt about $<110>$ (Physica **25**, 409-422, 1959, No. 6).

Small-angle grain boundaries are known to consist of arrays of dislocations. In this paper it is shown that in the diamond lattice not only for small, but for all angles of tilt about $[1\bar{1}0]$ a dislocation model can be constructed. There are no abrupt changes of model for small variations of the angle of tilt and the {111} twin boundary comes out automatically. This twin boundary can equally well be described as a twist boundary with a network of screw dislocations, but both models are identical with the generally accepted structure of the {111} twin boundary.

2728: M. J. Sparnaay: Van der Waals forces and fluctuation phenomena (Physica **25**, 444-454, 1959, No. 6).

An expression is given for the attraction between two electrically neutral systems each consisting of electric point charges which move at random inside spherical volumes. The calculation is based on the use of mean square values of density fluctuations in each system. The result and the method used are compared with Keesom's expression for the interaction between two dipoles and with the expression which is obtained for the interaction of two classical harmonic oscillators a large distance apart.

2729: P. H. J. A. Kleijnen: Travelling-wave-buizen (T. Ned. Radiogenootschap **24**, 71-88, 1959, No. 2/3). (Travelling-wave tubes; in Dutch.)

Fundamentals of the theory of the various forms of travelling-wave tube. The article substantially reproduces an introductory lecture given at the symposium on travelling-wave tubes organized by the Netherlands Radio Society in 1958.

2730: C. T. de Wit: Een 10-watt-lopendegolfbuis voor de 7,5-cm-band (T. Ned. Radiogenootschap **24**, 89-100, 1959, No. 2/3). (A 10-watt travelling-wave tube for the 7.5 cm waveband; in Dutch.)

Discussion of the main factors involved in the design and construction of a travelling-wave tube of high beam efficiency. An outline is given of the design of some of the components of the tube and of the circuit.

2731: A. Versnel: Lopendegolfbuizen met een laag ruisgetal (T. Ned. Radiogenootschap **24**, 101-112, 1959, No. 2/3). (Travelling-wave tubes with a low noise factor; in Dutch.)

The behaviour of current and velocity fluctuations in a travelling-wave tube are discussed. The calculations are done in 3 stages: first fluctuations between cathode and anode are considered, then the behaviour of these fluctuations in the drift space between anode and helical electrode and finally their behaviour when they interact with the signal injected on the helix. If the beam diameter, beam velocity in the drift space and beam current are kept constant, it is found that the noise factor depends only on the cathode-anode potential and on the length of the drift space. By a suitable choice of these parameters the minimum noise figure can be achieved. With certain assumptions, the calculated values agree with those measured on special laboratory tubes. It is shown that if certain conditions could be fulfilled it should be possible to achieve even lower noise factors.

2732: J. Ubbink: Masers, I (T. Ned. Radiogenootschap **24**, 129-136, 1959, No. 2/3; in Dutch).

Introductory article on the operation of the maser. Processes such as absorption and stimulated and spontaneous emission are discussed in connection with the inversion of energy-level population densities. This inversion (higher population in the higher

levels), often characterized by the term "negative temperature", is essential to maser operation. The reason why magnetic dipole systems are more favourable than electric dipole systems is outlined. It is also explained why low temperatures are favourable to maser operation. The product of amplification and bandwidth and the noise of a maser are discussed with the aid of an equivalent circuit.

2733: T. Kralt, H. D. Moed, E. J. Ariëns and Th. W. J. Hendriksen: Synthesis and pharmacological properties of O-acetylsalicylamides (Rec. Trav. chim. Pays-Bas **78**, 199-206, 1959, No. 3).

The synthesis of a series of N-substituted O-acetylsalicylamides is described. Most compounds possess weak antipyretic activity and strong spasmolytic activity.

2734: T. Kralt, H. D. Moed, E. J. Ariëns and Th. W. J. Hendriksen: Synthesis and pharmacological properties of salicylamides (Rec. Trav. chim. Pays-Bas **78**, 207-214, 1959, No. 3).

The synthesis of a series of N-substituted salicylamides is described. Most compounds possess weak antipyretic activity and strong spasmolytic activity.

2735: A. Venema: The production of ultra-high vacua by means of a diffusion pump (Vacuum **9**, 54-57, 1959, No. 1).

The result of a measurement of the so-called ultimate pressure of a diffusion pump is often not only determined by the pump itself, but also by the additional apparatus necessary for making this measurement. An analysis is given of the gases which may be present at the pump mouth and the factors determining the pressure of those gases are treated. A discussion of the methods which can be used for making these pressures as small as possible results in a design of a pump apparatus. A description of this apparatus, which includes a mercury diffusion pump with cooling traps, is given. With the apparatus a pump speed at the recipient of 5-10 l/s for the common gases is obtained and an ultimate pressure lower than 10^{-12} mm Hg is reached. (See also Philips tech. Rev. **20**, 145-157, 1958/59.)

R 387: J. van Laar and J. J. Scheer: Photoelectric determination of the electron work function of indium (Philips Res. Repts. **15**, 1-6, 1960, No. 1).

The photoelectric work function of evaporated indium films prepared in ultra-high vacuum is found to be 4.08 $\pm$ 0.01 eV.

R 388: C. Kooy and U. Enz: Experimental and theoretical study of the domain configuration in thin layers of $BaFe_{12}O_{19}$ (Philips Res. Repts. **15**, 7-29, 1960, No. 1).

With the aid of the optical Faraday effect the domain configuration and the magnetization process in thin transparent single-crystal plates of $BaFe_{12}O_{19}$ are studied. The plates have surfaces parallel to the basal plane of the hexagonal structure. The domain pattern consists of line-shaped domains. The domain width is measured as dependent on the applied magnetic field parallel to the c-axis. The width of a reversed domain decreases slowly with the applied field reaching a finite thickness near saturation, whereas the width of a domain magnetized in the direction of the applied field increases rapidly near saturation. In this stage the remaining reversed line-shaped domains contract towards cylindrical domains which collapse at slightly higher fields. Saturation is reached in a field well below $4\pi I_s$. The demagnetizing energy of a partly magnetized thin uniaxial crystal having the easy axis normal to the surface is calculated for a domain pattern consisting of straight parallel domains. The stable domain configuration for a given value of the magnetic field is obtained by minimizing the total energy. The solution is obtained in the form of two simultaneous equations containing the two different domain widths, which are evaluated by an electronic computer. Theoretical magnetization curves are deduced. The general accordance between experiment and theory is good.

R 389: K. Teer: Investigations into redundancy and possible bandwidth compression in television transmission (Philips Res. Repts. **15**, 30-96, 1960, No. 1).

Continuation of **R 385**.

R 390: M. E. Wise: On the radii of five packed spheres in mutual contact (Philips Res. Repts. **15**, 101-106, 1960, No. 2).

These results form part of a study of close packing in spheres. Each of four given spheres touches the other three. The fifth ("interstitial") sphere touches all four externally and is usually surrounded by them. The other sphere touching all four either lies outside them or encloses them. These properties are shown by geometrical inversion. In this way a general equation relating to the radii of five spheres in mutual contact is derived. Some general conclusions about different configurations of the five spheres are discussed on the basis of this relation. The formulae are also expressed in terms of statistical functions

of the four radii; the volume of the tetrahedron of centres of the first four spheres is shown to be related to the same functions.

R 391: F. van der Maesen: Determination of numbers of injected holes and electrons in semiconductors (Philips Res. Repts. **15**, 107-119, 1960, No. 2).

In semiconductors, deviations Δn and Δp of the equilibrium numbers n_0 and p_0 of electrons and holes are unequal in many cases because of trapping. It is shown how measurements of the photo Hall-effect and photoconduction may give information on the numbers Δn and Δp separately. From the ratio Y of the relative change of the Hall-effect and of the photoconductivity, the quantity $K = \Delta n/\Delta p$ can be evaluated. Graphs of Y versus K for some substances are given. It is shown how K occurs in the formulae used in computations of the diffusion-recombination length L from photoelectromagnetic and photoconductive data. If r_n and r_p denote the ratios of the Hall-mobility to drift mobility for electrons and holes, respectively, r_n/r_p can be evaluated from the measurements where $K = 1$. In this way the value of r_n/r_p at room temperature is found to be 0.54 ± 0.05 for germanium and 0.78 ± 0.04 for solicon.

R 392: C. A. A. J. Greebe and W. F. Knippenberg: Grown *p-n* junctions in silicon carbide (Philips Res. Repts **15**, 120-123, 1960, No. 2).

An account is given of the preparation and properties of grown junctions in SiC. The forward characteristics are tentatively explained on the basis of a *p-i-n* structure. *P-n* luminescence has been observed containing violet light.

R 393: M. T. Vlaardingerbroek: Small-signal performance and noise properties of microwave triodes (Philips Res. Repts. **15**, 124-221, 1960, No. 2).

This paper (thesis, Eindhoven 1959) reports on a theoretical and experimental study of the behaviour of a microwave triode at 4 Gc/s. After a general survey of the field, the equivalent circuit of the triode is deduced in section 2. The internal feedback is accounted for by a series-resonant circuit in the grid lead. The noise behaviour is described by a noise-current source and a noise-voltage source connected to the input terminals of the equivalent circuit. In section 3, those elements of the equivalent circuit which result from the presence of electrons in the active space and the noise sources are calculated on the basis of the single-velocity transit-time theory of Llewellyn and Petersen. Four phenomenological constants are introduced, to account for the effects of the electrons returning in front of the potential minimum and for the multi-velocity effects on the original "Rack" velocity fluctuation and the convection-current fluctuation at the cathode surface. The methods of measurement necessary for the determination of the fourpole coefficients of the triode and its four characteristic noise quantities, giving the magnitudes of the noise sources and their cross-correlation, are described in section 4. These methods are complicated because the distance between the measuring devices and the object under study is of the order of several wavelengths. In section 5 the experiments are described and the results are compared with the theory of sections 2 and 3. The conclusions are: (1) The electronic admittances of the triode can be calculated with reasonable accuracy on the basis of the single-velocity transit-time theory provided that the current density is so high that the distance from cathode to potential minimum is small compared to the cathode-grid distance. (2) The noise properties of the triode are only slightly affected by total-emission noise, transit-time spread and feedback. The contribution of reflection of electrons at the anode surface to the noise properties of a microwave triode is of some importance and can be estimated. (3) The random emission from the cathode is the most important noise source. The four measured noise quantities can be used for calculating the four phenomenological noise quantities introduced in section 3. From the values obtained for the latter quantities, the minimum noise figure and the beam-noise parameters S and Π of an electron-beam amplifier equipped with an identical cathode can be calculated. The results are in reasonable agreement with the measured values of S and Π.

R 394: G. Meijer and M. Avinor: Excitation spectra of vanadium-activated zinc and cadmium sulphide and selenide phosphors (Philips Res. Repts. **15**, 225-237, 1960, No. 3).

Excitation spectra were measured for the 2 μ fluorescence band of vanadium-activated zinc and cadmium sulphide and selenide phosphors. The emission is excited by absorption in two composite bands due to vanadium at 1.1 and 1.6 eV, by absorption in an auxiliary impurity centre, such as copper or silver, if present, and by fundamental excitation.

R 395: W. van Gool and A. P. Cleiren: Self-activated and Cu-activated fluorescence of ZnS (Philips Res. Repts. **15**, 238-253, 1960, No. 3).

Two series of experiments on the fluorescence of ZnS are described. The first one, of which only a review of the experimental results is given, presents some additional data on the theory of ZnS activated with Cu, made some years ago by Kröger and co-workers. In the second series a limited number of phosphors have been studied in order to settle a few questions. In particular, the difference between the blue Cu emission and the blue self-activated emission of ZnS has been studied. Furthermore, the temperature dependence of the fluorescence bands and the influence of the coactivator on both mentioned fluorescences and the green copper fluorescence were determined. The results can be interpreted by assuming that the low-temperature fluorescence is dependent on the coactivator. The room-temperature emission bands can have a composite character, in such a way that in addition to the low-temperature emission band another band may be important. The results are to some extent uncertain, due to experimental difficulties. These have been discussed and it is stressed that further careful experimental work may be more important for our knowledge of the ZnS fluorescence than detailed calculations about some special model.

R 396: W. van Gool, A. P. Cleiren and H. J. M. Heijligers: Fluorescence of some activated ZnS phosphors (Philips Res. Repts. **15**, 254-274, 1960, No. 3).

Several series of ZnS phosphors were prepared in H_2S atmosphere at 1150-1200 °C. Activators used were Ag, Cu, Au and coactivators were Al, Sc, Ga, In. Phosphors were made with all combinations of activators and coactivators with one concentration. In other phosphors equal concentrations of selected pairs of activators and coactivators were studied at different levels. Some special series of phosphors were made in addition, and spectral distributions of all phosphors at room temperature and at —196 °C are reported. The spectral distributions can be separated into parts of low and high photon energy. The high-energy parts can be attributed to the presence of the activators. The low-energy parts are of a composite structure. Part of these bands is due to an associate centre of activator and coactivator. Other parts of the low-energy bands may be due to other centres, which could not be identified unambiguously.

R 397: J. A. W. van der Does de Bye: Measurement of decay times of excess carriers in semiconductors, excited by X-ray pulses (Philips Res. Repts. **15**, 275-289, 1960, No. 3).

A method for the measurement of transient decay times of excess carrier concentrations in homogeneous semiconductors is described. The exciting agent is X-rays, which are delivered in short pulses of 0.1-0.3 μsec. A reasonable excitation (about 10^{12} cm^{-3} per pulse in Ge) requires peak currents of several tens of amperes through the X-ray tube, which is fitted with a large dispenser cathode. Two pulse generators, which can deliver short, high-tension pulses of 80 kV and of 150 kV, are used. These two voltages imply two different effective linear X-ray attenuation coefficients for every substance. For germanium they are about 20 cm^{-1} and 8 cm^{-1}. This affords a reasonable possibility of exciting the bulk without much disturbance by surface recombination. Excitation, dissipation, sample geometry and noise set a minimum to the resistivity of the sample for the production of a clearly visible decay curve on the oscilloscope. For Ge this is between 0.1 and 1 ohm cm. The measuring apparatus comprises an exponential time base and a decay-curve simulator for the measurements of decay time constants, down to 0.1 μsec. Measurements performed on copper-doped germanium yield decay times which are also found with chopped light. Some measurements on CdTe are also described.

R 398: H. G. Grimmeiss and H. Koelmans: *P-n* luminescence and photovoltaic effects in GaP (Philips Res. Repts. **15**, 290-304, 1960, No. 3).

GaP crystals were prepared from the elements. Crystals made at low phosphorus pressure mainly showed *n*-conductivity with an activation energy of 0.07 eV. Crystals with *p*-conductivity were obtained by heating at high phosphorus pressure (activation energy 0.19 eV) or by doping with Zn. The non-doped crystals showed electroluminescence in bands at 6250 Å and 5650 Å. The electroluminescence is shown to be due to the recombination of charge carriers, within *p-n* junctions via levels within the forbidden gap. A level scheme for undoped GaP is proposed. The crystals showed point-contact rectification and photovoltaic effects. On measuring the photovoltage as a function of wavelength, excitation bands were found at 4200 Å and 5600 Å in non-doped crystals and at 4200 Å and 6000 Å in Zn-doped crystals. The long-wave excitation peaks of the photovoltage are explained with a two-step mechanism, one optical and one thermal.